

Information Newton's flow: second-order optimization method in probability space

Yifei Wang^{*1} and Wuchen Li^{†2},

¹School of Mathematical Sciences, Peking University

²Department of Mathematics, UCLA

ABSTRACT. We introduce a framework for Newton's flows in probability space with information metrics, named information Newton's flows. Here two information metrics are considered, including both the Fisher-Rao metric and the Wasserstein-2 metric. Several examples of information Newton's flows for learning objective/loss functions are provided, such as Kullback-Leibler (KL) divergence, Maximum mean discrepancy (MMD), and cross entropy. The asymptotic convergence results of proposed Newton's methods are provided. A known fact is that overdamped Langevin dynamics correspond to Wasserstein gradient flows of KL divergence. Extending this fact to Wasserstein Newton's flows of KL divergence, we derive Newton's Langevin dynamics. We provide examples of Newton's Langevin dynamics in both one-dimensional space and Gaussian families. For the numerical implementation, we design sampling efficient variational methods to approximate Wasserstein Newton's directions. Several numerical examples in Gaussian families and Bayesian logistic regression are shown to demonstrate the effectiveness of the proposed method.

Keywords: Optimal transport; Information geometry; Langevin dynamics; Information Newton's flow; Newton's Langevin dynamics.

1. INTRODUCTION

Optimization problems in probability space are of great interest in inverse problems, information science, physics, and scientific computing, with applications in machine learning (Amari, 2016; Stuart, 2010; Liu, 2017; Amari, 1998; Villani, 2003). One typical problem here comes from Bayesian inference, which provides an optimal probability formulation for learning models from observed data. Given a prior distribution, the problem is to generate samples from a (target) posterior distribution (Stuart, 2010). From an optimization perspective, such a problem often refers to minimizing an objective function, such as the Kullback-Leibler (KL) divergence, in the probability space. The update relates to finding a sampling representation for the evolution of the probability.

In practice, one often needs to transfer probability optimization problems into sampling-based formulations, and then design efficient updates in the form of samples. Here first-order methods, such as gradient descent methods, play essential roles. We notice that gradient directions for samples rely on the metric over the probability space, which reflects the change of objective/loss functions. In practice, there are several important metrics, often named information metrics from information geometry and optimal transport, including the Fisher-Rao metric (Amari, 1998) and the Wasserstein-2 metric (in short, Wasserstein metric) (Otto, 2001; Lafferty, 1988). In literature, along with a given information metric,

^{*}zackwang24@pku.edu.cn

[†]wcli@math.ucla.edu

the probability space can be viewed as a Riemannian manifold, named density manifold (Lafferty, 1988).

For the Fisher-Rao metric, its gradient flow, known as birth-death dynamics, are important in modeling population games and designing evolutionary dynamics (Amari, 2016). It is also important for optimization problems in discrete probability (Malagò and Pistone, 2014) and machine learning (Ollivier et al., 2017). Recently, the Fisher-Rao gradient has also been applied for accelerating Bayesian sampling problems in continuous sample space (Lu et al., 2019). The Fisher-Rao gradient direction also inspires the design of learning algorithms for probability models. Several optimization methods in machine learning approximate the Fisher-Rao gradient direction, including the Kronecker-factored Approximate Curvature (K-FAC) (Martens and Grosse, 2015) method and adaptive estimates of lower-order moments (Adam) method (Kingma and Ba, 2014).

For the Wasserstein metric, its gradient direction deeply connects with stochastic differential equations and the associated Markov chain Monte Carlo methods (MCMC). An important fact is that the Wasserstein gradient of KL divergence forms the Kolmogorov forward generator of overdamped Langevin dynamics (Jordan et al., 1998). Hence, many MCMC methods can be viewed as Wasserstein gradient descent methods. In recent years, there are also several generalized Wasserstein metrics, such as Stein metric (Liu and Wang, 2016; Liu, 2017), Hessian transport (mobility) metrics (Carrillo et al., 2010; Dolbeault et al., 2009; Li and Ying, 2019) and Kalman-Wasserstein metric (Garbuno-Inigo et al., 2019). These metrics introduce various first-order methods with sampling efficient properties. For instance, the Stein variational gradient descent (Liu and Wang, 2016, SVGD) introduces a kernelized interacting Langevin dynamics. The Kalman-Wasserstein metric introduces a particular mean-field interacting Langevin dynamics (Garbuno-Inigo et al., 2019), known as ensemble Kalman sampling. On the other hand, many approaches design fast algorithms on modified Langevin dynamics. These methods can also be viewed and analyzed by the modified Wasserstein gradient descent, see details in (Ma et al., 2019; Simsekli et al., 2016; Li, 2019). By viewing sampling as optimization problems in the probability space, many efficient sampling algorithms are inspired by classical optimization methods. E.g., Bernton (2018); Wibisono (2019) apply the operator splitting technique to improve the unadjusted Langevin algorithm. Liu et al. (2018); Taghvaei and Mehta (2019); Wang and Li (2019) study Nesterov’s accelerated gradient methods in probability space.

In optimization, the Newton’s method is a fundamental second-order method to accelerate optimization computations. For optimization problems in probability space, several natural questions arise: *Can we systematically design Newton’s methods to accelerate sampling related optimization problems? What is the Newton’s flow in probability space under information metrics? Focusing on the Wasserstein metric, can we extend the relation between Wasserstein gradient flow of KL divergence and Langevin dynamics? In other words, what is the Wasserstein Newton’s flow of KL divergence and which Langevin dynamics does it corresponds to?*

In this paper, following (Li, 2018; Wang and Li, 2019), we complete these questions. We derive Newton’s flows in probability space with general information metrics. By studying these Newton’s flows, we provide the convergence analysis. Focusing on Wasserstein Newton’s flows of KL divergence, we derive several analytical examples in one-dimensional

space and Gaussian families. Besides, we design two algorithms as particle implementations of Wasserstein Newton’s flows in high dimensional sample space. This is to restrict the dual variable (cotangent vector) associated with Newton’s direction into a finite-dimensional affine function space. A hybrid update of Newton’s direction and gradient direction is also introduced. For the concreteness of presentation, we demonstrate the Wasserstein Newton’s flow of KL divergence in Theorem 1.

Theorem 1 (Wasserstein Newton’s flow of KL divergence). *Given a target density $\rho^*(x) \propto \exp(-f(x))$, where f is a given function, denote the KL divergence between ρ and ρ^* by*

$$D_{KL}(\rho\|\rho^*) = \int \rho \log \frac{\rho}{e^{-f}} dx - \log Z, \quad (1)$$

where $Z = \int \exp(-f(x)) dx$. Then the Wasserstein Newton’s flow of KL divergence follows

$$\partial_t \rho_t + \nabla \cdot (\rho_t \nabla \Phi_t^{\text{Newton}}) = 0, \quad (2)$$

where Φ_t^{Newton} satisfies the following equation

$$\nabla^2 : (\rho_t \nabla^2 \Phi_t) - \nabla \cdot (\rho_t \nabla^2 f \nabla \Phi_t) - \nabla \cdot (\rho_t \nabla f) - \Delta \rho_t = 0. \quad (3)$$

Here we notice that Φ_t^{Newton} is the solution to the Wasserstein Newton’s direction equation (3). In Figure 1, we provide a sampling (particle) formulation of Wasserstein Newton’s flows. We compare formulations among Wasserstein Newton’s flows, Wasserstein gradient flows and overdamped Langevin dynamics.

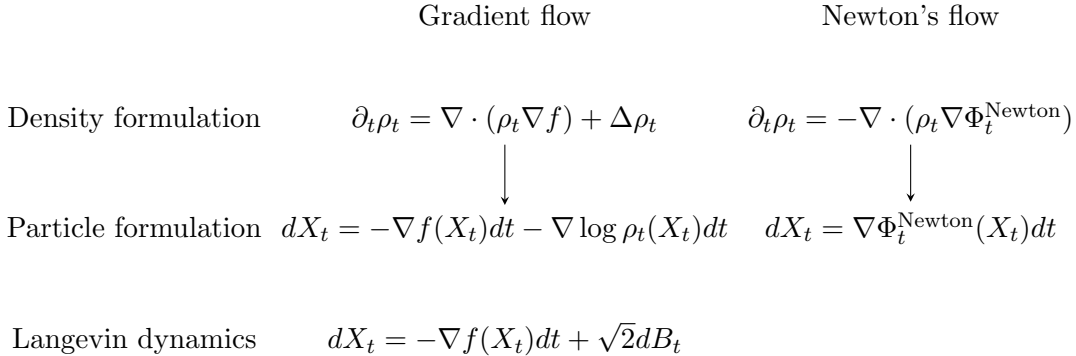


FIGURE 1. The relation among Wasserstein gradient flow, Newton’s flow and Langevin dynamics. Our approach derive the particle formulation of Wasserstein Newton’s flow of KL divergence.

In literature, second-order methods are developed for optimization problems on Riemannian manifold, see (Smith, 1994; Yang, 2007). Here we are interested in density manifold, i.e., probability space with information metrics. Compared to known results in Riemannian optimization, we not only develop methods in probability space but also find efficient sampling representations of the algorithms. In discrete probability simplex with Fisher-Rao metric and exponential family models, the Newton’s method has also been studied by (Malagò and Pistone, 2014), known as the second order method in information geometry. Also, Detommaso et al. (2018); Chen et al. (2019) design second-order methods for the Stein variational gradient descent direction. Our approach generalizes these

results to information metrics, especially for the Wasserstein metric. On the other hand, the Newton-type MCMC method has been studied in (Simsekli et al., 2016), known as Hessian Approximated MCMC (HAMCMC) method. The differences between HAMCMC and our proposed Newton’s Langevin dynamics can be observed from evolutions in probability space. HAMCMC utilizes the Hessian matrix of logarithm of target density function and derives the associated drift-diffusion process. In density space, it is still a linear local partial differential equation (PDE). Newton’s Langevin dynamics apply the Hessian operator of KL divergence based on the Wasserstein metric. In density space, the Wasserstein Newton’s flow is a nonlocal PDE. A careful comparison of all related Langevin dynamics in analytical (subsection 4.2) and numerical examples (subsection 8.1 8.2) are provided.

We organize this paper as follows. In section 2, we briefly review information metrics and corresponding gradient operators in probability space. We introduce properties of Hessian operators and derive various forms of Newton’s flows for different objective functions in section 3. Focusing on Wasserstein Newton’s flows of KL divergence, we formulate the Newton’s direction equation in one-dimensional sample space (see section 4) and Gaussian families (see section 5). In section 6, the asymptotic convergence rate of Newton’s method is proved. Two sampling efficient numerical algorithms are presented in section 7. Several numerical examples for sampling problems are provided in section 8.

2. REVIEW ON NEWTON’S FLOWS AND INFORMATION METRICS

In this section, we briefly review Newton’s methods and Newton’s flows in Euclidean spaces and Riemannian manifolds. Then, we focus on a probability space, in which we introduce information metrics with the associated gradient and Hessian operators. Based on them, we will derive the Newton’s flow under information metrics later on. Throughout this paper, we use $\langle \cdot, \cdot \rangle$ and $\| \cdot \|$ to denote the Euclidean inner product and norm in \mathbb{R}^n .

2.1. Finite dimensional Newton’s flow. We first briefly review Newton’s methods and Newton’s flows in Euclidean spaces. Given an objective function $f: \mathbb{R}^n \rightarrow \mathbb{R}$, consider an optimization problem:

$$\min_{x \in \mathbb{R}^n} f(x).$$

The update rule of the (damped) Newton’s method follows

$$x_{k+1} = x_k + \alpha_k p_k, \quad p_k = -(\nabla^2 f(x_k))^{-1} \nabla f(x_k).$$

Here $\alpha_k > 0$ is a step size and p_k is called the Newton’s direction. With $\alpha_k = 1$, we recover the classical Newton’s methods. By taking a limit $\alpha_k \rightarrow 0$, the Newton’s method in continuous-time, namely Newton’s flow, writes

$$\dot{x} = -(\nabla^2 f(x))^{-1} \nabla f(x). \quad (\text{Euclidean Newton’s flow})$$

We next consider an optimization problem on a Riemannian manifold $\mathcal{M} \subset \mathbb{R}^n$. Given an objective function $f: \mathcal{M} \rightarrow \mathbb{R}$, consider

$$\min_{x \in \mathcal{M}} f(x).$$

The tangent space $T_x \mathcal{M}$ and the cotangent space $T_x^* \mathcal{M}$ at x are identical to a linear subspace of \mathbb{R}^n . For $p, q \in T_x \mathcal{M}$, let $\langle p, q \rangle_x = p^T \mathcal{G}(x) q$ denote an inner product in tangent space $T_x \mathcal{M}$ at x . Here $\mathcal{G}(x)$ is called the metric tensor, which corresponds to a symmetric semi-positive definite matrix in $\mathbb{R}^{n \times n}$. For the Euclidean case, we can view

$T_x\mathcal{M} = T_x^*\mathcal{M} = \mathbb{R}^n$ and $\mathcal{G}(x) = I$, where I is an identity matrix. The Riemannian gradient of f at x is the unique tangent vector v such that the following equality holds for all $p \in T_x\mathcal{M}$.

$$\langle \text{grad } f(x), p \rangle_x = \lim_{\epsilon \rightarrow 0} \frac{f(x + \epsilon p) - f(x)}{\epsilon}.$$

The Riemannian Hessian of f at x is a linear mapping from $T_x\mathcal{M}$ to $T_x\mathcal{M}$ defined by

$$\text{Hess } f(x)p = \nabla_p \text{grad } f(x), \quad \forall p \in T_x\mathcal{M}.$$

Here $\nabla_p \text{grad } f(x)$ is the covariant derivative of $\text{grad } f(x)$ w.r.t. the tangent vector p . Detailed definitions of gradient and Hessian operators on a Riemannian manifold can be found in (Huang, 2013, Chapter 1). The update rule of the Newton's method writes

$$x_{k+1} = R_{x_k}(\alpha_k p_k), \quad p_k = -(\text{Hess } f(x_k))^{-1} \text{grad } f(x_k).$$

Here R_{x_k} can be the exponential mapping or the retraction (first-order approximation of the exponential mapping) at x_k . Based on the Riemannian metric of \mathcal{M} , the exponential mapping uniquely maps a tangent vector to a point in \mathcal{M} along the geodesic curve. Different from the Euclidean case, the update of x_{k+1} is based on the (approximated) geodesic curve of \mathcal{M} . In continuous time, the Newton's flow follows

$$\dot{x} = -(\text{Hess } f(x))^{-1} \text{grad } f(x). \quad (\text{Riemannian Newton's flow})$$

Example 1 (Rayleigh's quotient on a sphere). *Let $\mathcal{M} = S^{n-1} \subset \mathbb{R}^n$ be a unit sphere in \mathbb{R}^n and $f(x) = x^T A x$, where A is a symmetric matrix. Minimizing $f(x)$ is equivalent to finding the eigenvector corresponding to A 's smallest eigenvalue. The tangent space and the cotangent space of \mathcal{M} follow*

$$T_x\mathcal{M} = T_x^*\mathcal{M} = \{p \in \mathbb{R}^n : p^T x = 0\}.$$

The inner product $\langle p, q \rangle_x = p^T q$ is identical to the Euclidean inner product in \mathbb{R}^n . Based on previous definitions, we derive

$$\text{grad } f(x) = 2Ax - 2f(x)x, \quad \text{Hess } f(x)p = 2(I - xx^T)(A - f(x)I)p.$$

If $(A - f(x)I)$ is invertible, then the inverse of the Hessian operator writes

$$(\text{Hess } f(x))^{-1}p = \frac{1}{2}(A - f(x)I)^{-1} \left(q - \frac{x^T(A - f(x)I)^{-1}p}{x^T(A - f(x)I)^{-1}x} x \right).$$

The exponential map at x with direction p satisfies

$$\text{Exp}_x(p) = x \cos(\|p\|) + \frac{p}{\|p\|} \sin(\|p\|), \quad p \in T_x S^{n-1}.$$

Hence, the update rule of the Newton's method in S^{n-1} follows

$$\begin{cases} x_{k+1} = x_k \cos(\|p_k\|) + \frac{p_k}{\|p_k\|} \sin(\|p_k\|), \\ p_k = -x_k + \frac{(A - f(x_k)I)^{-1}x_k}{x_k^T(A - f(x_k)I)^{-1}x_k}. \end{cases}$$

From now on, we consider optimization problems in probability space. Suppose that sample space Ω is a region in \mathbb{R}^n . Let $\mathcal{F}(\Omega)$ represent the set of smooth functions on Ω . Denote the set of probability density

$$\mathcal{P}(\Omega) = \left\{ \rho \in \mathcal{F}(\Omega) : \int_{\Omega} \rho dx = 1, \quad \rho \geq 0. \right\}.$$

The optimization problem in $\mathcal{P}(\Omega)$ takes the form:

$$\min_{\rho \in \mathcal{P}(\Omega)} E(\rho).$$

Here $E(\rho)$ is the objective or loss functional. It evaluates certain divergence or metric functional between ρ and a target density $\rho^* \in \mathcal{P}(\Omega)$. In machine learning problems, typical examples of $E(\rho)$ include the KL divergence, Maximum mean discrepancy (MMD), cross entropy, etc. Similar to (Euclidean Newton's flow) and (Riemannian Newton's flow), the Newton's flow in probability space (density manifold) takes the form

$$\partial_t \rho_t = -(\text{Hess } E(\rho_t))^{-1} \text{grad } E(\rho_t). \quad (\text{Information Newton's flow})$$

Here grad and Hess represent the gradient and the Hessian operator with respect to certain information metric, respectively. To understand (Information Newton's flow), we briefly review the information metrics with the associated gradient operators.

2.2. Information metrics. We first define the tangent space and the cotangent space in probability space. The tangent space at $\rho \in \mathcal{P}(\Omega)$ is defined by

$$T_\rho \mathcal{P}(\Omega) = \left\{ \sigma \in \mathcal{F}(\Omega) : \int \sigma dx = 0. \right\}.$$

The cotangent space $T_\rho^* \mathcal{P}(\Omega)$ is equivalent to $\mathcal{F}(\Omega)/\mathbb{R}$, which represents the set of functions in $\mathcal{F}(\Omega)$ defined up to addition of constants.

Definition 1 (Metric in probability space). *For a given $\rho \in \mathcal{P}(\Omega)$, a metric tensor $\mathcal{G}(\rho) : T_\rho \mathcal{P}(\Omega) \rightarrow T_\rho^* \mathcal{P}(\Omega)$ is an invertible mapping from the tangent space $T_\rho \mathcal{P}(\Omega)$ to the cotangent space $T_\rho^* \mathcal{P}(\Omega)$. This metric tensor defines the metric (inner product) on the tangent space $T_\rho \mathcal{P}(\Omega)$. Namely, for $\sigma_1, \sigma_2 \in T_\rho \mathcal{P}(\Omega)$, we define the inner product $g_\rho : T_\rho \mathcal{P}(\Omega) \times T_\rho \mathcal{P}(\Omega) \rightarrow \mathbb{R}$ by*

$$g_\rho(\sigma_1, \sigma_2) = \int \sigma_1 \mathcal{G}(\rho) \sigma_2 dx = \int \Phi_1 \mathcal{G}(\rho)^{-1} \Phi_2 dx,$$

where Φ_i is the solution to $\sigma_i = \mathcal{G}(\rho)^{-1} \Phi_i$, $i = 1, 2$.

We present two essential examples of metrics in probability space $\mathcal{P}(\Omega)$: Fisher-Rao metric and Wasserstein metric.

Example 2 (Fisher-Rao metric). *The inverse of the Fisher-Rao metric tensor follows*

$$\mathcal{G}^F(\rho)^{-1} \Phi = \rho \left(\Phi - \int \Phi \rho dx \right), \quad \Phi \in T_\rho^* \mathcal{P}(\Omega).$$

The Fisher-Rao metric is defined by

$$g_\rho^F(\sigma_1, \sigma_2) = \int \Phi_1 \Phi_2 \rho dx - \left(\int \Phi_1 \rho dx \right) \left(\int \Phi_2 \rho dx \right), \quad \sigma_1, \sigma_2 \in T_\rho \mathcal{P}(\Omega),$$

where Φ_i is the solution to $\sigma_i = \rho (\Phi_i - \int \Phi_i \rho dx)$, $i = 1, 2$.

Example 3 (Wasserstein metric). *The inverse of the Wasserstein metric tensor satisfies*

$$\mathcal{G}^W(\rho)^{-1} \Phi = -\nabla \cdot (\rho \nabla \Phi), \quad \Phi \in T_\rho^* \mathcal{P}(\Omega).$$

The Wasserstein metric is given by

$$g_\rho^W(\sigma_1, \sigma_2) = \int \rho \langle \nabla \Phi_1, \nabla \Phi_2 \rangle dx, \quad \sigma_1, \sigma_2 \in T_\rho \mathcal{P}(\Omega),$$

where Φ_i is the solution to $\sigma_i = -\nabla \cdot (\rho \nabla \Phi_i)$, $i = 1, 2$.

2.3. Gradient operators. The gradient operator for the objective functional $E(\rho)$ in $(\mathcal{P}(\Omega), \mathcal{G}(\rho))$ satisfies

$$\text{grad } E(\rho) = -\mathcal{G}(\rho)^{-1} \frac{\delta E}{\delta \rho}.$$

Here $\frac{\delta E}{\delta \rho}$ is the L^2 first variation w.r.t. ρ . The gradient flow follows

$$\partial_t \rho_t = -\text{grad } E(\rho_t) = -\mathcal{G}(\rho)^{-1} \frac{\delta E}{\delta \rho_t}.$$

We present gradient operators under either Fisher-Rao metric or Wasserstein metric.

Example 4 (Fisher-Rao gradient operator). *The Fisher-Rao gradient operator satisfies*

$$\text{grad}^F E(\rho) = \rho \left(\frac{\delta E}{\delta \rho} - \int \frac{\delta E}{\delta \rho} \rho dx \right).$$

The Fisher-Rao gradient flow follows

$$\partial_t \rho_t = -\text{grad}^F E(\rho) = -\rho_t \left(\frac{\delta E}{\delta \rho_t} - \int \frac{\delta E}{\delta \rho_t} \rho_t dx \right).$$

Example 5 (Wasserstein gradient operator). *The Wasserstein gradient operator writes*

$$\text{grad}^W E(\rho) = -\nabla \cdot \left(\rho \nabla \frac{\delta E}{\delta \rho} \right).$$

The Wasserstein gradient flow satisfies

$$\partial_t \rho_t = -\text{grad}^W E(\rho) = \nabla \cdot \left(\rho_t \nabla \frac{\delta E}{\delta \rho_t} \right).$$

3. INFORMATION NEWTON'S FLOW

In this section, we introduce and discuss properties of Hessian operators in probability space. Then, we formulate Newton's flows under information metrics. This is based on the previous definition of gradient operators and the inverse of Hessian operators.

3.1. Information Hessian operators. In this subsection, we review the definition of Hessian operators in probability space and provide the exact formulations of Hessian operators.

For $\sigma \in T_\rho \mathcal{P}(\Omega)$, there exists a unique geodesic curve $\hat{\rho}_s$, which satisfies $\hat{\rho}_s|_{s=0} = \rho$ and $\hat{\partial}_s \rho_s|_{s=0} = \sigma$. The Hessian operator of $E(\rho)$ w.r.t. metric tensor $\mathcal{G}(\rho)$ is a mapping $\text{Hess } E(\rho) : T_\rho \mathcal{P}(\Omega) \rightarrow T_\rho \mathcal{P}(\Omega)$, which is defined by

$$g_\rho(\text{Hess } E(\rho)\sigma, \sigma) = g_\rho(\sigma, \text{Hess } E(\rho)\sigma) = \frac{d^2}{ds^2} E(\hat{\rho}_s) \Big|_{s=0}.$$

We briefly review the concept of self-adjoint operator.

Definition 2 (Self-adjoint). *Suppose that V is a Hilbert space and let $\mathcal{H} : V \rightarrow V^*$ be a linear operator. V^* is the adjoint space of V , which consists of all linear functionals on V . Let $(f, v) = (v, f) = f(v)$ denote the coupling of $v \in V$ and $f \in V^*$. The adjoint operator of \mathcal{H} is the unique linear operator $\mathcal{H}^* : V \rightarrow V^*$, which satisfies*

$$(\mathcal{H}v_1, v_2) = (v_1, \mathcal{H}^*v_2), \quad \forall v_1, v_2 \in V.$$

We say that \mathcal{H} is self-adjoint if $\mathcal{H} = \mathcal{H}^*$.

Remark 1. *If $V = \mathbb{R}^n$ is the Euclidean space, then the linear operator \mathcal{H} can be viewed as a matrix in $\mathbb{R}^{n \times n}$. Then, to say that \mathcal{H} is self-adjoint operator is equivalent to say that \mathcal{H} is a symmetric matrix.*

Combining with the metric tensor, the Hessian operator uniquely defines a self-adjoint mapping $\mathcal{H}_E(\rho) : T_\rho^*\mathcal{P}(\Omega) \rightarrow T_\rho\mathcal{P}(\Omega)$, which satisfies

$$\int \Phi \mathcal{H}_E(\rho) \Phi dx = g_\rho(\sigma, \text{Hess } E(\rho)\sigma), \quad \Phi = \mathcal{G}(\rho)\sigma.$$

In Proposition 1, we give an exact formulation of $\int \Phi \mathcal{H}_E(\rho) \Phi dx$ and a relationship between $\mathcal{H}_E(\rho)$ and $\text{Hess } E(\rho)$.

Proposition 1. *The quantity $g_\rho(\sigma, \text{Hess } E(\rho)\sigma)$ is a bi-linear form of Φ :*

$$\begin{aligned} \int \Phi \mathcal{H}_E(\rho) \Phi dx &= g_\rho(\sigma, \text{Hess } E(\rho)\sigma) \\ &= -\frac{1}{2} \int \mathcal{A}(\rho)(\Phi, \Phi) \mathcal{G}(\rho)^{-1} \frac{\delta E}{\delta \rho} dx + \int \mathcal{A}(\rho) \left(\Phi, \frac{\delta E}{\delta \rho} \right) \mathcal{G}(\rho)^{-1} \Phi dx \quad (4) \\ &\quad + \int \int (\mathcal{G}(\rho)^{-1} \Phi)(y) \frac{\delta^2 E}{\delta \rho^2}(x, y) dy (\mathcal{G}(\rho)^{-1} \Phi)(x) dx. \end{aligned}$$

Here $\frac{\delta^2 E}{\delta \rho^2}(x, y)$ is defined by

$$\frac{\delta^2 E}{\delta \rho^2}(x, y) = \frac{\delta}{\delta \rho} \left(\int \frac{\delta E}{\delta \rho}(y) \delta(x - y) dy \right),$$

where $\delta(x)$ is the Dirac delta function. Here $\mathcal{A}(\rho) : T_\rho^*\mathcal{P}(\Omega) \times T_\rho^*\mathcal{P}(\Omega) \rightarrow T_\rho^*\mathcal{P}(\Omega)$ is a bi-linear operator which satisfies

$$\mathcal{A}(\rho)(\Phi_1, \Phi_2) = \frac{\delta}{\delta \rho} \int \Phi_1 \mathcal{G}(\rho)^{-1} \Phi_2 dx, \quad \forall \Phi_1, \Phi_2 \in T_\rho^*\mathcal{P}(\Omega).$$

Moreover, the operator $\mathcal{H}_E(\rho)$ satisfies

$$\mathcal{H}_E(\rho) = \text{Hess } E(\rho) \mathcal{G}(\rho)^{-1}. \quad (5)$$

Proof. The geodesic curve $\hat{\rho}_s$ satisfies geodesic equation

$$\begin{cases} \partial_s \hat{\rho}_s - \mathcal{G}(\hat{\rho}_s)^{-1} \Phi_s = 0, \\ \partial_s \Phi_s + \frac{1}{2} \frac{\delta}{\delta \hat{\rho}_s} \left(\int \Phi_s \mathcal{G}(\hat{\rho}_s)^{-1} \Phi_s dx \right) = 0, \end{cases} \quad (6)$$

with initial values $\hat{\rho}_s|_{s=0} = \rho$ and $\Phi_s|_{s=0} = \Phi$. For the first-order derivative, it follows

$$\frac{d}{ds} E(\hat{\rho}_s) = \int \partial_s \hat{\rho}_s \frac{\delta E}{\delta \hat{\rho}_s} dx = \int \Phi_s \mathcal{G}(\hat{\rho}_s)^{-1} \frac{\delta E}{\delta \hat{\rho}_s} dx,$$

where we utilize the fact that $\mathcal{G}(\hat{\rho}_s)$ is self-adjoint. For the second-order derivative,

$$\begin{aligned} \frac{d^2}{ds^2}E(\hat{\rho}_s) &= \int \partial_s \Phi_s \mathcal{G}(\hat{\rho}_s)^{-1} \frac{\delta E}{\delta \hat{\rho}_s} dx + \int \partial_s \hat{\rho}_s \frac{\delta}{\delta \hat{\rho}_s} \left(\frac{d}{ds} E(\hat{\rho}_s) \right) dx \\ &= -\frac{1}{2} \int \mathcal{A}(\hat{\rho}_s)(\Phi_s, \Phi_s) \mathcal{G}(\hat{\rho}_s)^{-1} \frac{\delta E}{\delta \hat{\rho}_s} dx + \int \mathcal{A}(\hat{\rho}_s) \left(\Phi_s, \frac{\delta E}{\delta \hat{\rho}_s} \right) \mathcal{G}(\hat{\rho}_s)^{-1} \Phi_s dx \\ &\quad + \int \int (\mathcal{G}(\hat{\rho}_s)^{-1} \Phi_s)(y) \frac{\delta^2 E}{\delta \hat{\rho}_s^2}(x, y) (\mathcal{G}(\hat{\rho}_s)^{-1} \Phi_s)(x) dx dy. \end{aligned}$$

Based on the definition of $\mathcal{H}_E(\rho)$, (4) is proved by setting $s = 0$ in the above formula. To prove (5), we introduce Lemma 1.

Lemma 1. *Let \mathcal{H} be a self-adjoint linear operator from $T_\rho^* \mathcal{P}(\Omega) \rightarrow T_\rho \mathcal{P}(\Omega)$. Namely $\mathcal{H}^* = \mathcal{H}$. Suppose that $\int \Phi \mathcal{H} \Phi dx = 0$ for all $\Phi \in T_\rho^* \mathcal{P}(\Omega)$. Then, $\mathcal{H} = 0$.*

Proof. Because \mathcal{H} is self-adjoint and linear, for any $\Phi \in T_\rho^* \mathcal{P}(\Omega)$, it follows

$$\mathcal{H} \Phi = \frac{1}{2} \frac{\delta}{\delta \Phi} \int \Phi \mathcal{H} \Phi dx = 0,$$

which completes the proof. \square

Note that $\text{Hess } E(\rho)$ is self-adjoint w.r.t. the metric tensor $G(\rho)$, namely

$$(\text{Hess } E(\rho))^* \mathcal{G}(\rho) = \mathcal{G}(\rho) \text{Hess } E(\rho), \quad \mathcal{G}(\rho)^{-1} (\text{Hess } E(\rho))^* = \text{Hess } E(\rho) \mathcal{G}(\rho)^{-1}.$$

where $(\text{Hess } E(\rho))^*$ is the adjoint operator of $\text{Hess } E(\rho)$. This tells that $\text{Hess } E(\rho) \mathcal{G}(\rho)^{-1}$ is self-adjoint. We have the following relationship.

$$\int \Phi \mathcal{H}_E(\rho) \Phi dx = g_\rho(\text{Hess } E(\rho) \sigma, \sigma) = \int \Phi \mathcal{G}(\rho)^{-1} \text{Hess } E(\rho) \Phi dx.$$

As a direct result of Lemma 2, it follows $\mathcal{H}_E(\rho) = \text{Hess } E(\rho) \mathcal{G}(\rho)^{-1}$. \square

For simplicity, we define positive definite operators as follows.

Definition 3. *Suppose that V is a Hilbert space and let $\mathcal{H} : V \rightarrow V^*$ be a self-adjoint linear operator. We say that \mathcal{H} is positive definite, if $(\mathcal{H}v, v) > 0$ for all $v \in V, v \neq 0$.*

Proposition 2 provides a sufficient condition to ensure that the Hessian operator is injective (invertible).

Proposition 2. *Suppose that $g_\rho(\text{Hess } E(\rho) \sigma, \sigma) > 0$ for all $\sigma \neq 0, \sigma \in T_\rho \mathcal{P}(\Omega)$. Namely, $\mathcal{H}_E(\rho)$ is positive definite. Then, $\text{Hess } E(\rho)$ is injective.*

Proof. If there exist $\sigma_1, \sigma_2 \in T_\rho \mathcal{P}(\Omega)$ such that $\text{Hess } E(\rho) \sigma_1 = \text{Hess } E(\rho) \sigma_2$. Then,

$$g_\rho((\sigma_1 - \sigma_2), \text{Hess } E(\rho) (\sigma_1 - \sigma_2)) = \int (\sigma_1 - \sigma_2) G(\rho)^{-1} \text{Hess } E(\rho) (\sigma_1 - \sigma_2) dx = 0,$$

By our assumption $g_\rho(\text{Hess } E(\rho) \sigma, \sigma) > 0$ for all $\sigma \neq 0$, we have $\sigma_1 = \sigma_2$. \square

The inverse of the Hessian operator $\text{Hess } E(\rho)$ follows

$$(\text{Hess } E(\rho))^{-1} \sigma = \mathcal{G}(\rho)^{-1} \mathcal{H}_E(\rho)^{-1} \sigma,$$

or equivalently,

$$(\text{Hess } E(\rho))^{-1} \mathcal{G}(\rho)^{-1} \Phi = \mathcal{G}(\rho)^{-1} \mathcal{H}_E(\rho)^{-1} \mathcal{G}(\rho)^{-1} \Phi.$$

Now, we are ready to present the Newton's flow in probability space, named information Newton's flow.

Proposition 3 (Information Newton's flow). *The Newton's flow of objective function $E(\rho)$ in $(\mathcal{P}(\Omega), \mathcal{G}(\rho))$ satisfies*

$$\partial_t \rho_t + (\text{Hess } E(\rho_t))^{-1} \mathcal{G}(\rho_t)^{-1} \frac{\delta E}{\delta \rho_t} = 0.$$

This is equivalent to

$$\begin{cases} \partial_t \rho_t - \mathcal{G}(\rho_t)^{-1} \Phi_t = 0, \\ \mathcal{H}_E(\rho_t) \Phi_t + \mathcal{G}(\rho_t)^{-1} \frac{\delta}{\delta \rho_t} E(\rho_t) = 0. \end{cases} \quad (7)$$

We next show several examples of Newton's flows under either Fisher-Rao metric or Wasserstein metric.

3.2. Newton's flows under Fisher-Rao metric. For Fisher-Rao metric, the geodesic curve $\hat{\rho}_s$ satisfies

$$\begin{cases} \partial_s \hat{\rho}_s - \rho_s \left(\Phi_s - \int \Phi_s \hat{\rho}_s dy \right) = 0, \\ \partial_s \Phi_s + \frac{1}{2} \Phi_s^2 - \left(\int \Phi_s \hat{\rho}_s dy \right) \Phi_s = 0. \end{cases}$$

And the bi-linear operator $\mathcal{A}^F(\rho)$ follows

$$\mathcal{A}^F(\rho)(\Phi_1, \Phi_2) = \Phi_1 \Phi_2 - \left(\int \Phi_2 \rho dy \right) \Phi_1 - \left(\int \Phi_1 \rho dy \right) \Phi_2. \quad (8)$$

For simplicity, we let $\mathbb{E}_\rho[\Phi] = \int \Phi \rho dx$, where $\Phi \in T_\rho^* \mathcal{P}(\Omega)$.

Proposition 4 (Fisher-Rao Newton's flow). *For an objective function $E : \mathcal{P}(\Omega) \rightarrow \mathbb{R}$, the Fisher-Rao Newton's flow follows*

$$\begin{cases} \partial_t \rho_t - \rho_t (\Phi_t - \mathbb{E}_{\rho_t}[\Phi_t]) = 0, \\ \mathcal{H}_E^F(\rho_t) \Phi_t - \rho_t \left(\frac{\delta E}{\delta \rho_t} - \mathbb{E}_{\rho_t} \left[\frac{\delta E}{\delta \rho_t} \right] \right) = 0, \end{cases} \quad (9)$$

where $\mathcal{H}_E^F(\rho) : T_\rho^* \mathcal{P}(\Omega) \rightarrow T_\rho \mathcal{P}(\Omega)$ defines a bi-linear form: for $\Phi \in T_\rho^* \mathcal{P}(\Omega)$,

$$\begin{aligned} \int \Phi \mathcal{H}_E^F(\rho) \Phi dx &= \frac{1}{2} \int \mathcal{A}^F(\rho) \left(\Phi, \frac{\delta E}{\delta \rho} \right) (\Phi - \mathbb{E}_\rho[\Phi]) \rho dx \\ &+ \int \int \rho(y) (\Phi(y) - \mathbb{E}_\rho[\Phi]) \frac{\delta^2 E}{\delta \rho^2}(x, y) dy \rho(x) (\Phi(x) - \mathbb{E}_\rho[\Phi]) dx. \end{aligned} \quad (10)$$

Proof. Based on Proposition 1, we only need to prove that

$$\int \mathcal{A}^F(\rho)(\Phi, \Phi) \mathcal{G}^F(\rho)^{-1} \frac{\delta E}{\delta \rho} dx = \int \mathcal{A}^F(\rho) \left(\Phi, \frac{\delta E}{\delta \rho} \right) \mathcal{G}^F(\rho)^{-1} \Phi dx.$$

The left hand side follows

$$\begin{aligned}
& \int \mathcal{A}^F(\rho)(\Phi, \Phi) \mathcal{G}^F(\rho)^{-1} \frac{\delta E}{\delta \rho} dx \\
&= \int (\Phi^2 - 2\mathbb{E}_\rho[\Phi]\Phi) \left(\frac{\delta E}{\delta \rho} - \mathbb{E}_\rho \left[\frac{\delta E}{\delta \rho} \right] \right) \rho dx \\
&= \int (\Phi - \mathbb{E}_\rho[\Phi]) \left(\frac{\delta E}{\delta \rho} - \mathbb{E}_\rho \left[\frac{\delta E}{\delta \rho} \right] \right) \Phi \rho dx - \mathbb{E}_\rho[\Phi] \int \left(\frac{\delta E}{\delta \rho} - \mathbb{E}_\rho \left[\frac{\delta E}{\delta \rho} \right] \right) \Phi \rho dx.
\end{aligned}$$

The right hand side satisfies

$$\begin{aligned}
& \int \mathcal{A}^F(\rho) \left(\Phi, \frac{\delta E}{\delta \rho} \right) \mathcal{G}^F(\rho)^{-1} \Phi dx \\
&= \int \left(\Phi \frac{\delta E}{\delta \rho} - \mathbb{E}_\rho \left[\frac{\delta E}{\delta \rho} \right] \Phi - \mathbb{E}_\rho[\Phi] \frac{\delta E}{\delta \rho} \right) (\Phi - \mathbb{E}_\rho[\Phi]) \rho dx \\
&= \int (\Phi - \mathbb{E}_\rho[\Phi]) \left(\frac{\delta E}{\delta \rho} - \mathbb{E}_\rho \left[\frac{\delta E}{\delta \rho} \right] \right) \Phi \rho dx - \mathbb{E}_\rho[\Phi] \int \frac{\delta E}{\delta \rho} (\Phi - \mathbb{E}_\rho[\Phi]) \rho dx.
\end{aligned}$$

We also observe that

$$\int \frac{\delta E}{\delta \rho} (\Phi - \mathbb{E}_\rho[\Phi]) \rho dx = \mathbb{E}_\rho \left[\Phi \frac{\delta E}{\delta \rho} \right] - \mathbb{E}_\rho[\Phi] \mathbb{E}_\rho \left[\frac{\delta E}{\delta \rho} \right] = \int \left(\frac{\delta E}{\delta \rho} - \mathbb{E}_\rho \left[\frac{\delta E}{\delta \rho} \right] \right) \Phi \rho dx.$$

Hence, the left hand side is equal to the right hand side. \square

Example 6 (Fisher-Rao Newton's flow of KL divergence). *Suppose that $E(\rho)$ evaluates the KL divergence from ρ to $\rho^* \sim \exp(-f)$. This objective functional also writes*

$$E(\rho) = \int (\rho \log \rho + f \rho) dx.$$

We derive that

$$\frac{\delta E}{\delta \rho}(x) = \log \rho(x) + f + 1, \quad \frac{\delta^2 E}{\delta \rho^2}(x, y) = \frac{\delta(x - y)}{\rho(y)}.$$

Based on Proposition 4, we can compute that (4) is equivalent to

$$\begin{aligned}
\int \Phi \mathcal{H}_E(\rho) \Phi dx &= \frac{1}{2} \int (\Phi^2 - 2\mathbb{E}_\rho[\Phi]\Phi) (\log \rho + f - \mathbb{E}_\rho[\log \rho + f]) \rho dx \\
&\quad + \int (\Phi(x) - \mathbb{E}_\rho[\Phi]) \rho(x) \int \frac{\delta(y - x)}{\rho(y)} (\Phi(y) - \mathbb{E}_\rho[\Phi]) \rho(y) dy dx \\
&= \frac{1}{2} \int (\log \rho + f - \mathbb{E}_\rho[\log \rho + f]) \Phi^2 \rho dx \\
&\quad - \mathbb{E}_\rho[\Phi] \int (\log \rho + f - \mathbb{E}_\rho[\log \rho + f]) \Phi \rho dx \\
&\quad + \int \Phi^2 \rho dx - \left(\int \Phi \rho dx \right)^2.
\end{aligned}$$

Hence, the operator $\mathcal{H}_E^F(\rho)$ follows

$$\begin{aligned}\mathcal{H}_E^F(\rho)\Phi &= \frac{1}{2}(\log \rho + f - \mathbb{E}_\rho[\log \rho + f])\Phi\rho - \frac{1}{2}\left(\int(\log \rho + f - \mathbb{E}_\rho[\log \rho + f])\Phi\rho dy\right)\rho \\ &\quad - \frac{1}{2}\mathbb{E}_\rho[\Phi](\log \rho + f - \mathbb{E}_\rho[\log \rho + f])\rho + \Phi\rho - \mathbb{E}_\rho[\Phi]\rho \\ &= \frac{1}{2}(2 + \log \rho + f - \mathbb{E}_\rho[\log \rho + f])(\Phi - \mathbb{E}_\rho[\Phi])\rho \\ &\quad - \frac{1}{2}(\mathbb{E}_\rho[\Phi(\log \rho + f)] - \mathbb{E}_\rho[\Phi]\mathbb{E}_\rho[(\log \rho + f)])\rho.\end{aligned}$$

Example 7 (Fisher-Rao Newton's flow of interaction energy). *Consider an interaction energy*

$$E(\rho) = \frac{1}{2} \int \int \rho(x)W(x, y)\rho(y)dx dy,$$

where $W(x, y) = W(y, x)$ is a kernel function. The interaction energy also formulates the MMD, see details in (Gretton et al., 2012). We can compute that

$$\frac{\delta E}{\delta \rho}(x) = \int W(x, y)\rho(y)dy, \quad \frac{\delta^2 E}{\delta \rho^2}(x, y) = W(x, y).$$

We denote $(W * \rho)(x) = \int W(x, y)\rho(y)dx$. Based on Proposition 4, it follows

$$\begin{aligned}&\int \Phi \mathcal{H}_E^F(\rho)\Phi dx \\ &= \frac{1}{2} \int (\Phi^2 - 2\mathbb{E}_\rho[\Phi]\Phi)(W * \rho - \mathbb{E}_\rho[W * \rho])\rho dx \\ &\quad + \int \int (\Phi(y) - \mathbb{E}_\rho[\Phi])W(x, y)\rho(y)\rho(x)(\Phi(x) - \mathbb{E}_\rho[\Phi])dy dx \\ &= \frac{1}{2} \int \Phi^2(W * \rho - \mathbb{E}_\rho[W * \rho])\rho dx - \mathbb{E}_\rho[\Phi] \left(\int \Phi(W * \rho - \mathbb{E}_\rho[W * \rho])\rho dx \right) \\ &\quad + \int \int \Phi(x)\rho(x)W(x, y)\Phi(y)\rho(y)dx dy + (\mathbb{E}_\rho[\Phi])^2 \left(\int \int \rho(x)W(x, y)\rho(y)dx dy \right) \\ &\quad - 2\mathbb{E}_\rho[\Phi] \left(\int \int \rho(x)W(x, y)\Phi(x)\rho(y)dx dy \right).\end{aligned}$$

Hence, the operator $\mathcal{H}_E^F(\rho)$ satisfies

$$\begin{aligned}\mathcal{H}_E^F(\rho)\Phi(x) &= \frac{1}{2}(W * \rho - \mathbb{E}_\rho[W * \rho])\rho\Phi - \frac{1}{2}\left(\int \Phi(W * \rho - \mathbb{E}_\rho[W * \rho])\rho dy\right)\rho \\ &\quad - \frac{1}{2}\mathbb{E}_\rho[\Phi](W * \rho - \mathbb{E}_\rho[W * \rho])\rho + (W * (\rho\Phi))\rho \\ &\quad + \mathbb{E}_\rho[W * \rho]\mathbb{E}_\rho[\Phi]\rho - \mathbb{E}_\rho[W * (\rho\Phi)]\rho - \mathbb{E}_\rho[\Phi](W * \rho)\rho \\ &= \frac{1}{2}(W * \rho - \mathbb{E}_\rho[W * \rho])(\Phi - \mathbb{E}_\rho[\Phi])\rho - \frac{1}{2}(\mathbb{E}_\rho[\Phi(W * \rho)] - \mathbb{E}_\rho[\Phi]\mathbb{E}_\rho[W * \rho])\rho \\ &\quad + (W * (\rho\Phi) - \mathbb{E}_\rho[W * (\rho\Phi)])\rho - \mathbb{E}_\rho[\Phi]((W * \rho) - \mathbb{E}_\rho[W * \rho])\rho.\end{aligned}$$

Example 8 (Fisher-Rao Newton's flow of cross entropy). *Suppose that $E(\rho)$ is the cross entropy, i.e., reverse KL divergence. It evaluates the KL divergence from a given density*

ρ^* to ρ

$$E(\rho) = - \int \log \left(\frac{\rho}{\rho^*} \right) \rho^* dx = - \int (\log \rho) \rho^* dx + \int (\log \rho^*) \rho^* dx.$$

It is equivalent to optimize $E(\rho) = - \int (\log \rho) \rho^* dx$. We compute that

$$\frac{\delta E}{\delta \rho}(x) = -\frac{\rho^*(x)}{\rho(x)}, \quad \frac{\delta^2 E}{\delta \rho^2}(x, y) = \frac{\rho^*(y)}{\rho^2(y)} \delta(x - y).$$

Proposition 4 indicates that

$$\begin{aligned} \int \Phi \mathcal{H}_E^F(\rho) \Phi dx &= \frac{1}{2} \int (\Phi^2 - 2\mathbb{E}_\rho[\Phi]\Phi)(-\rho^*/\rho + \mathbb{E}_\rho[\rho^*/\rho])\rho dx \\ &\quad + \int (\Phi(x) - \mathbb{E}_\rho[\Phi])\rho(x) \int \frac{\rho^*(y)}{\rho^2(y)} \delta(x - y)(\Phi(y) - \mathbb{E}_\rho[\Phi])\rho(y) dy dx \\ &= \frac{1}{2} \int \Phi^2(\rho - \rho^*) dx - \mathbb{E}_\rho[\Phi] \int \Phi(\rho - \rho^*) dx + \int (\Phi - \mathbb{E}_\rho[\Phi])^2 \rho^* dx \\ &= \frac{1}{2} (\mathbb{E}_\rho[\Phi^2] - \mathbb{E}_{\rho^*}[\Phi^2]) - \mathbb{E}_\rho[\Phi](\mathbb{E}_\rho[\Phi] - \mathbb{E}_{\rho^*}[\Phi]) \\ &\quad + \mathbb{E}_{\rho^*}[\Phi^2] - 2\mathbb{E}_\rho[\Phi]\mathbb{E}_{\rho^*}[\Phi] + (\mathbb{E}_\rho[\Phi])^2 \\ &= \frac{1}{2} (\mathbb{E}_\rho[\Phi^2] + \mathbb{E}_{\rho^*}[\Phi^2]) - \mathbb{E}_\rho[\Phi]\mathbb{E}_{\rho^*}[\Phi]. \end{aligned}$$

Hence, the operator $\mathcal{H}_E^F(\rho)$ follows

$$\mathcal{H}_E^F(\rho)\Phi = \frac{1}{2} ((\Phi - \mathbb{E}_{\rho^*}[\Phi])\rho + (\Phi - \mathbb{E}_\rho[\Phi])\rho^*).$$

3.3. Newton's flows under Wasserstein metric. For Wasserstein metric, the geodesic curve $\hat{\rho}_s$ satisfies

$$\begin{cases} \partial_s \hat{\rho}_s + \nabla \cdot (\hat{\rho}_s \nabla \Phi_s) = 0, \\ \partial_s \Phi_s + \frac{1}{2} \|\nabla \Phi_s\|^2 = 0. \end{cases}$$

The bi-linear operator $\mathcal{A}^W(\rho)$ follows

$$\mathcal{A}^W(\rho)(\Phi_1, \Phi_2) = \langle \nabla \Phi_1, \nabla \Phi_2 \rangle.$$

Proposition 5 (Wasserstein Newton's flow). *For an objective functional $E: \mathcal{P}(\Omega) \rightarrow \mathbb{R}$, the Wasserstein Newton's flow follows*

$$\begin{cases} \partial_t \rho_t + \nabla \cdot (\rho_t \nabla \Phi_t) = 0, \\ \mathcal{H}_E^W(\rho_t)\Phi_t - \nabla \cdot \left(\rho_t \nabla \frac{\delta E}{\delta \rho_t} \right) = 0. \end{cases} \quad (11)$$

Here $\mathcal{H}_E(\rho): T_\rho^* \mathcal{P}(\Omega) \rightarrow T_\rho \mathcal{P}(\Omega)$ defines a bi-linear form: for $\Phi \in T_\rho^* \mathcal{P}(\Omega)$,

$$\begin{aligned} \int \Phi \mathcal{H}_E^W(\rho) \Phi dx &= \int \int \left\langle \nabla \Phi(x), \nabla_x \nabla_y \frac{\delta^2 E}{\delta \rho^2}(x, y) \nabla \Phi(y) \right\rangle \rho(x) \rho(y) dx dy \\ &\quad + \int \left\langle \nabla \Phi, \nabla^2 \frac{\delta E}{\delta \rho} \nabla \Phi \right\rangle \rho dx. \end{aligned} \quad (12)$$

Proof. Based on integration by parts, we observe that

$$\begin{aligned}
& \int \mathcal{A}^W(\rho)(\Phi, \Phi) \mathcal{G}^W(\rho)^{-1} \frac{\delta E}{\delta \rho} dx \\
&= - \int \|\nabla \Phi\|^2 \nabla \cdot \left(\rho \nabla \frac{\delta E}{\delta \rho} \right) dx \\
&= \int \left\langle \nabla \frac{\delta E}{\delta \rho}, \nabla \|\nabla \Phi\|^2 \right\rangle \rho dx \\
&= 2 \int \left\langle \nabla \frac{\delta E}{\delta \rho}, \nabla^2 \Phi \nabla \Phi \right\rangle \rho dx,
\end{aligned}$$

and

$$\begin{aligned}
& \int \mathcal{A}^W(\rho) \left(\Phi, \frac{\delta E}{\delta \rho} \right) \mathcal{G}^W(\rho)^{-1} \Phi dx \\
&= - \int \left\langle \nabla \Phi, \nabla \frac{\delta E}{\delta \rho} \right\rangle \nabla \cdot (\rho \nabla \Phi) dx \\
&= \int \left\langle \nabla \left\langle \nabla \Phi, \nabla \frac{\delta E}{\delta \rho} \right\rangle, \nabla \Phi \right\rangle \rho dx \\
&= \int \left\langle \nabla \Phi, \nabla^2 \Phi \nabla \frac{\delta E}{\delta \rho} \right\rangle \rho dx + \int \left\langle \nabla \Phi, \nabla^2 \frac{\delta E}{\delta \rho} \nabla \Phi \right\rangle \rho dx.
\end{aligned}$$

Combining above two observations with Proposition 1, we derive

$$\begin{aligned}
\int \Phi \mathcal{H}_E^W(\rho) \Phi dx &= \int \left\langle \nabla \Phi, \nabla^2 \frac{\delta E}{\delta \rho} \nabla \Phi \right\rangle \rho dx \\
&+ \int \int \nabla \cdot (\rho \nabla \Phi)(y) \frac{\delta^2 E}{\delta \rho^2}(x, y) \nabla \cdot (\rho \nabla \Phi)(x) dx dy \\
&= \int \int \left\langle \nabla \Phi(x), \nabla_x \nabla_y \frac{\delta^2 E}{\delta \rho^2}(x, y) \nabla \Phi(y) \right\rangle \rho(x) \rho(y) dx dy \\
&+ \int \left\langle \nabla \Phi, \nabla^2 \frac{\delta E}{\delta \rho} \nabla \Phi \right\rangle \rho dx.
\end{aligned}$$

This proves Proposition 5. \square

Example 9 (Wasserstein Newton's flow of KL divergence). *In this example we prove Theorem 1. As a known fact in (Otto and Villani, 2000) and Gamma calculus (Bakry and Émery, 1985; Li, 2018), the Hessian operator of KL divergence under the Wasserstein metric follows*

$$g_\rho^W(\sigma, \text{Hess}^W E(\rho)\sigma) = \int \left(\|\nabla^2 \Phi\|_F^2 + (\nabla \Phi)^T \nabla^2 f \nabla \Phi \right) \rho dx,$$

where $\sigma = -\nabla \cdot (\rho \nabla \Phi)$ and $\|\cdot\|_F$ is the Frobenius norm of a matrix in $\mathbb{R}^{n \times n}$. Via integration by parts, we validate that the operator $\mathcal{H}_E^W(\rho)$ follows

$$\mathcal{H}_E^W(\rho)\Phi = \nabla^2 : (\rho \nabla^2 \Phi) - \nabla \cdot (\rho \nabla^2 f \nabla \Phi). \quad (13)$$

Example 10 (Wasserstein Newton's flow of interaction energy). *Consider an interaction energy*

$$E(\rho) = \frac{1}{2} \int \int \rho(x) W(x, y) \rho(y) dx dy.$$

Combining with previous computations, Proposition 5 yields that

$$\begin{aligned} \int \Phi \mathcal{H}_E^W(\rho) \Phi dx &= \int \int \langle \nabla \Phi(x), \nabla_x \nabla_y W(x, y) \nabla \Phi(y) \rangle \rho(x) \rho(y) dx dy \\ &\quad + \int \left\langle \nabla \Phi(x), \int \nabla_x^2 W(x, y) \rho(y) dy \nabla \Phi(x) \right\rangle \rho(x) dx \\ &= \frac{1}{2} \mathbb{E}_{x, y \sim \rho} \begin{bmatrix} \nabla \Phi(x) \\ \nabla \Phi(y) \end{bmatrix}^T \begin{bmatrix} \nabla_{xx}^2 W(x, y) & \nabla_{xy}^2 W(x, y) \\ \nabla_{yx}^2 W(x, y) & \nabla_{yy}^2 W(x, y) \end{bmatrix} \begin{bmatrix} \nabla \Phi(x) \\ \nabla \Phi(y) \end{bmatrix}. \end{aligned}$$

Based on integration by parts, the operator $\mathcal{H}_E^W(\rho)$ is given by

$$\mathcal{H}_E^W(\rho) \Phi = -\nabla \cdot (\rho(\nabla_{xy}^2 W * (\rho \nabla \Phi))) - \nabla \cdot (\rho(\nabla_{xx}^2 W * \rho) \nabla \Phi).$$

Example 11 (Wasserstein Newton's flow of cross entropy). Suppose that $E(\rho)$ evaluates the KL divergence from a given density ρ^* to ρ

$$E(\rho) = -\int \log \left(\frac{\rho}{\rho^*} \right) \rho^* dx = -\int (\log \rho) \rho^* dx + \int (\log \rho^*) \rho^* dx.$$

It is equivalent to optimize $E(\rho) = -\int (\log \rho) \rho^* dx$. Proposition 5 yields

$$\begin{aligned} \int \Phi \mathcal{H}_E^W(\rho) \Phi dx &= \int \nabla \cdot (\rho(x) \nabla \Phi(x)) \int \frac{\rho^*(y)}{\rho^2(y)} \delta(x-y) \nabla \cdot (\rho(y) \nabla \Phi(y)) dy dx \\ &\quad - \int \left\langle \nabla \Phi(x), \nabla_x^2 \left(\frac{\rho^*(x)}{\rho(x)} \right) \nabla \Phi(x) \right\rangle \rho(x) dx \\ &= \int (\rho^{-1} \nabla \cdot (\rho \nabla \Phi))^2 \rho^* dx - \int \left\langle \nabla \Phi, \nabla^2 \left(\frac{\rho^*}{\rho} \right) \nabla \Phi \right\rangle \rho dx. \end{aligned}$$

Hence, the operator $\mathcal{H}_E^W(\rho)$ satisfies

$$\mathcal{H}_E^W(\rho) \Phi = \nabla \cdot \left(\rho \nabla \left(\frac{\rho^*}{\rho^2} \nabla \cdot (\rho \nabla \Phi) \right) \right) + \nabla \cdot \left(\rho \nabla^2 \left(\frac{\rho^*}{\rho} \right) \nabla \Phi \right).$$

Remark 2. For simplicity of presentations, we only present the Hessian formulas for Fisher-Rao and Wasserstein information metrics. In fact, there are many interesting generalized Hessian formulas in Li (2019) from Hessian transport metrics. We leave systematic studies of Newton's flows for general metrics in future works.

4. NEWTON'S LANGEVIN DYNAMICS

In this section, we primarily focus on the Wasserstein Newton's flow of KL divergence. We formulate it into the Newton's Langevin dynamics for Bayesian sampling problems. The connection and difference with Newton's flows in Euclidean space and Hessian Approximated MCMC (HAMCMC) method (Simsekli et al., 2016) are discussed.

Let the objective functional $E(\rho) = \text{D}_{\text{KL}}(\rho \| \rho^*)$ evaluate the KL divergence from ρ to a target density $\rho^*(x) \propto \exp(-f(x))$ with $\int \exp(-f(x)) dx < \infty$. This specific optimization problem is important since it corresponds to sampling from the target density ρ^* . Classical Langevin MCMC algorithms evolves samples following overdamped Langevin dynamics (OLD), which satisfies

$$dX_t = -\nabla f(X_t) dt + \sqrt{2} dB_t,$$

where B_t is the standard Brownian motion. Denote ρ_t as the density function of the distribution of X_t . The evolution of ρ_t satisfies the Fokker-Planck equation

$$\partial_t \rho_t = \nabla \cdot (\rho_t \nabla f) + \Delta \rho_t.$$

A known fact is that the Fokker-Planck equation is the Wasserstein gradient flow (WGF) of KL divergence, i.e.

$$\begin{aligned} \partial_t \rho_t &= -\text{grad}^W \text{D}_{\text{KL}}(\rho_t \| \rho^*) \\ &= \mathcal{G}^W(\rho_t)^{-1} \frac{\delta}{\delta \rho_t} \text{D}_{\text{KL}}(\rho_t \| \rho^*) \\ &= \nabla \cdot (\rho_t \nabla (f + \log \rho_t + 1)) \\ &= \nabla \cdot (\rho_t \nabla f) + \Delta \rho_t. \end{aligned} \tag{14}$$

where we use the fact that $\frac{\delta}{\delta \rho} \text{D}_{\text{KL}}(\rho_t \| \rho^*) = \log \rho + t + f + 1$ and $\rho \nabla \log \rho = \nabla \rho$.

It is worth mentioning that OLD can be viewed as particle implementations of WGF (14). From the viewpoint of fluid dynamics, WGF also has a Lagrangian formulation

$$dX_t = -\nabla f(X_t) dt - \nabla \log \rho_t(X_t) dt.$$

We name above dynamics by the Lagrangian Langevin Dynamics (LLD). Here ‘Lagrangian’ refers to the Lagrangian coordinates (flow map) in fluid dynamics (Villani, 2008).

Overall, many sampling algorithms follow OLD or LLD. The evolution of corresponding density follows the Wasserstein gradient flow (14). E.g. the classical Langevin MCMC (unadjusted Langevin algorithm) is the time discretization of OLD. The Particle-based Variational Inference methods (ParVI), (Liu et al., 2019) can be viewed as the discrete-time approximation of LLD.

In short, we notice that the Langevin dynamics can be viewed as first-order methods for Bayesian sampling problems. Analogously, we derive the Wasserstein Newton’s flow of KL divergence in Example 9. It corresponds to certain Langevin dynamics of particle systems, named *Newton’s Langevin dynamics*.

Theorem 2. *Consider the Newton’s Langevin dynamics*

$$dX_t = \nabla \Phi_t^{\text{Newton}}(X_t) dt, \tag{15}$$

where $\Phi_t^{\text{Newton}}(x)$ is the solution to Wasserstein Newton’s direction equation (3):

$$\nabla^2 : (\rho_t \nabla^2 \Phi_t) - \nabla \cdot (\rho_t \nabla^2 f \nabla \Phi_t) - \nabla \cdot (\rho_t \nabla f) - \Delta \rho_t = 0.$$

Here X_0 follows an initial distribution ρ^0 and ρ_t is the distribution of X_t . Then, ρ_t is the solution to Wasserstein Newton’s flow with an initial value $\rho_0 = \rho^0$.

Proof. Note that ρ_t is the distribution of X_t . The dynamics of X_t implies

$$\partial_t \rho_t + \nabla \cdot (\rho_t \nabla \Phi_t^{\text{Newton}}) = 0.$$

Because Φ_t satisfies the Wasserstein Newton’s direction equation (3), ρ_t is the solution to Wasserstein Newton’s flow. \square

Remark 3. *We notice that the Newton’s Langevin dynamics is different from HAMCMC (Simsekli et al., 2016). HAMCMC approximates the dynamics of*

$$dX_t = -(\nabla^2 f(X_t))^{-1} (\nabla f(X_t) + \Gamma(X_t)) dt + \sqrt{2\nabla^2 f(X_t)^{-1}} dB_t,$$

where $\Gamma_i(x) = \sum_{j=1} \frac{\partial}{\partial x_j} \left((\nabla^2 f(X_t))^{-1} \right)_{i,j}$. Here $\Gamma(x)$ is a correction term to ensure that ρ_t converges to ρ^* . The evolution of ρ_t follows

$$\partial_t \rho_t = \nabla \cdot \left(((\nabla^2 f)^{-1} \nabla f + \Gamma) \rho_t \right) + \nabla^2 : ((\nabla^2 f)^{-1} \rho_t).$$

We formulate the above equation as

$$\partial_t \rho_t = \nabla \cdot (\rho_t (\nabla^2 f)^{-1} (\nabla f + \nabla \log \rho_t)) = \nabla \cdot (\rho_t \mathbf{v}_t), \quad (16)$$

where we denote $\mathbf{v}_t = (\nabla^2 f)^{-1} (\nabla f + \nabla \log \rho_t)$. Moreover, \mathbf{v}_t satisfies

$$-\nabla \cdot (\rho_t \nabla^2 f \mathbf{v}_t) - \nabla \cdot (\rho_t \nabla f) - \Delta \rho_t = 0.$$

On the other hand, replacing $\nabla \Phi_t^{\text{Newton}}$ by $\mathbf{v}_t^{\text{Newton}}$ in the Newton's direction equation (3) yields

$$\nabla^2 : (\rho_t \nabla \mathbf{v}_t^{\text{Newton}}) - \nabla \cdot (\rho_t \nabla^2 f \mathbf{v}_t^{\text{Newton}}) - \nabla \cdot (\rho_t \nabla f) - \Delta \rho_t = 0.$$

Hence, $\mathbf{v}_t \neq \mathbf{v}_t^{\text{Newton}}$. Then, (16) is different from information Newton's flow because the term $\nabla^2 : (\rho_t \nabla \mathbf{v}_t^{\text{Newton}})$ is not considered.

4.1. Connections and differences with Newton's flows in Euclidean space. We recall that the density evolution of particle's gradient flow in Euclidean space corresponds to the Wasserstein gradient flow (Villani, 2008). We notice that this relationship does not hold for the Wasserstein Newton's flow.

Consider an objective function:

$$E(\rho) = \int \rho(x) f(x) dx,$$

where $f(x)$ is a given smooth function. Here we notice that minimize ρ for $E(\rho)$ in probability space is equivalent to minimize x for $f(x)$ in Euclidean space. Namely, the support of the optimal solution ρ contains all global minimizers of $f(x)$. The gradient flow in Euclidean space of each particle follows

$$dX_t = -\nabla f(X_t) dt,$$

A known fact is that the density evolution of particles satisfies the following continuity equation

$$\partial_t \rho_t = \nabla \cdot (\rho_t \nabla f) = -\text{grad}^W E(\rho_t),$$

which is the Wasserstein gradient flow of $E(\rho)$ in probability space.

We next show that Newton's flow in Euclidean space of each particle does not coincide with the Wasserstein Newton's flow in probability space. For simplicity, we assume that $f(x)$ is strictly convex so $\nabla^2 f(x)$ is invertible for all x . Here, the Euclidean Newton's flow of each particle follows

$$dX_t = -(\nabla^2 f(X_t))^{-1} \nabla f(X_t) dt.$$

The density evolution of particles satisfies the continuity equation

$$\partial_t \rho_t = \nabla \cdot (\rho_t (\nabla^2 f)^{-1} \nabla f). \quad (17)$$

On the other hand, the Wasserstein Newton's flow writes

$$\partial_t \rho_t + \nabla \cdot (\rho_t \nabla \Phi_t^{\text{Newton}}) = 0, \quad (18)$$

where Φ_t^{Newton} is the unique solution to

$$-\nabla \cdot (\rho_t \nabla^2 f \nabla \Phi) - \nabla \cdot (\rho_t \nabla f) = 0. \quad (19)$$

We note that in general equation (17) can be different from equation (18). Later on in Lemma 2, we formulate the following Hodge decomposition of the Euclidean Newton's direction

$$-(\nabla^2 f)^{-1} \nabla f = \nabla \Phi_t^{\text{Newton}} + \xi_t,$$

where $\nabla \cdot (\rho_t \nabla^2 f \xi_t) = 0$. Here, the constraint on ξ_t does not necessarily ensure that $\nabla \cdot (\rho_t \xi_t) = 0$. Hence, equation (17) can be different from equation (18).

Remark 4. *In one dimensional case or f is a quadratic function, there exists Φ^{Newton} , such that $-(\nabla^2 f)^{-1} \nabla f = \nabla \Phi^{\text{Newton}}$. Hence equation (17) is same as equation (18). We also show an example that $\xi \neq 0$. Let $\Omega = \mathbb{R}^2$ and we define*

$$f(x) = \log(\exp(x_1) + \exp(x_2)) + \frac{\lambda}{2}(x_1^2 + x_2^2),$$

where $\lambda > 0$ is a parameter. For simplicity, we denote $p_1 = \exp(x_1)/(\exp(x_1) + \exp(x_2))$ and $p_2 = \exp(x_2)/(\exp(x_1) + \exp(x_2))$. Then, we can compute that the gradient and Hessian of $f(x)$ follows

$$\nabla f(x) = \begin{bmatrix} p_1 + \lambda x_1 \\ p_2 + \lambda x_2 \end{bmatrix}, \quad \nabla^2 f(x) = \begin{bmatrix} p_1 p_2 + \lambda & -p_1 p_2 \\ -p_1 p_2 & p_1 p_2 + \lambda \end{bmatrix}.$$

Because $p_1 p_2 + \lambda > 0$ and $\det(\nabla^2 f(x)) = \lambda^2 + 2\lambda p_1 p_2 > 0$, $\nabla^2 f(x)$ is positive definite. We note that

$$\begin{aligned} (\nabla^2 f(x))^{-1} \nabla f(x) &= \frac{1}{\lambda^2 + 2\lambda p_1 p_2} \begin{bmatrix} p_1 p_2 + \lambda & p_1 p_2 \\ p_1 p_2 & p_1 p_2 + \lambda \end{bmatrix} \begin{bmatrix} p_1 + \lambda x_1 \\ p_2 + \lambda x_2 \end{bmatrix} \\ &= \frac{1}{\lambda^2 + 2\lambda p_1 p_2} \begin{bmatrix} p_1 p_2 (1 + \lambda(x_1 + x_2)) + \lambda(p_1 + \lambda x_1) \\ p_1 p_2 (1 + \lambda(x_1 + x_2)) + \lambda(p_2 + \lambda x_2) \end{bmatrix} \\ &=: \begin{bmatrix} F_1(x) \\ F_2(x) \end{bmatrix}. \end{aligned}$$

If $(\nabla^2 f(x))^{-1} \nabla f(x)$ is a gradient vector field, we shall have

$$\partial_{x_2} F_1(x) = \partial_{x_1} F_2(x).$$

However, we can examine that

$$\begin{aligned} \partial_{x_2} F_1(x) &= \frac{p_1 p_2}{\lambda + 2p_1 p_2} \left(1 + p_1(1 + \lambda(x_1 + x_2)) + \frac{2\lambda p_1(\lambda(p_1 + \lambda x_1) + p_1 p_2(1 + \lambda(x_1 + x_2)))}{\lambda^2 + 2\lambda p_1 p_2} \right). \\ \partial_{x_1} F_2(x) &= \frac{p_1 p_2}{\lambda + 2p_1 p_2} \left(1 + p_2(1 + \lambda(x_1 + x_2)) + \frac{2\lambda p_2(\lambda(p_2 + \lambda x_2) + p_1 p_2(1 + \lambda(x_1 + x_2)))}{\lambda^2 + 2\lambda p_1 p_2} \right). \end{aligned}$$

This indicates that $(\nabla^2 f(x))^{-1} \nabla f(x)$ is not a gradient vector field. Hence, $\xi \neq 0$.

Lemma 2. *For given $\rho \in \mathcal{P}(\mathbb{R}^n)$, there exists a unique $\Phi \in T_\rho^* \mathcal{P}(\mathbb{R}^n)$ (up to a constant shrift) and a vector field $\xi : \mathbb{R}^n \rightarrow \mathbb{R}^n$ satisfying $\nabla \cdot (\rho \nabla^2 f \xi) = 0$ such that*

$$-(\nabla^2 f(x))^{-1} \nabla f(x) = \nabla \Phi(x) + \xi(x).$$

Proof. We first show the existence of $\Phi \in T_\rho^* \mathcal{P}(\mathbb{R}^n)$ and ξ . Note that Φ is the solution to

$$-\nabla \cdot (\rho \nabla^2 f \nabla \Phi) = \nabla \cdot (\rho \nabla f).$$

Denote $\mathcal{H}\Phi = -\nabla \cdot (\rho \nabla^2 f \nabla \Phi)$. Then, for $\Phi \neq 0$, we have

$$\int \Phi \mathcal{H}\Phi dx = \int \nabla \Phi^T \nabla^2 f \nabla \Phi \rho dx > 0.$$

Hence, \mathcal{H} is a positive definite operator and it is invertible. Thus $\Phi = \mathcal{H}^{-1}(\nabla \cdot (\rho \nabla f))$ exists. Because $\nabla^2 f \xi = \nabla f - \nabla^2 f \nabla \Phi$, it follows

$$\nabla \cdot (\nabla^2 f \xi) = \nabla \cdot (\rho \nabla f) - \nabla \cdot (\rho \nabla^2 f \nabla \Phi) = 0.$$

Hence, ξ also exists. We next prove the uniqueness. Suppose that $\nabla^2 f(x)^{-1} \nabla f(x) = \nabla \Phi_1(x) + \xi_1(x) = \nabla \Phi_2(x) + \xi_2(x)$. Then, we have $\nabla \Phi_1 - \nabla \Phi_2 = \xi_2 - \xi_1$. Hence

$$\begin{aligned} \int (\Phi_1 - \Phi_2) \mathcal{H}(\Phi_1 - \Phi_2) dx &= \int (\nabla \Phi_1 - \nabla \Phi_2)^T \nabla^2 f (\nabla \Phi_1 - \nabla \Phi_2) \rho dx \\ &= \int (\nabla \Phi_1 - \nabla \Phi_2)^T \nabla^2 f (\xi_2 - \xi_1) \rho dx = - \int (\Phi_1 - \Phi_2) \nabla \cdot (\rho \nabla^2 f (\xi_2 - \xi_1)) dx = 0. \end{aligned}$$

Because \mathcal{H} is positive definite, this yields that $\Phi_1 - \Phi_2 = 0$ (up to a spatial constant). \square

4.2. Newton's Langevin dynamics in one dimensional sample space. In this subsection, we provide examples of Newton's Langevin dynamics in one dimensional sample space. In particular, similar to the OrnsteinUhlenbeck (OU) process in classical Langevin dynamics, we derive a closed form solution to Newton's OU process.

Here we assume that $\Omega = \mathbb{R}$ and f is strictly convex. The essence of Newton's Langevin dynamics is to compute Φ_t^{Newton} from the Wasserstein Newton's direction equation (3). Proposition 2 ensures the uniqueness of the solution to (3). For the simplicity of notations, we neglect the subscript t .

Proposition 6. *Suppose that $\rho > 0$ and let $u = \nabla \Phi$. Then, the Newton's direction equation (3) reduces to an ODE*

$$u'' + u'(\log \rho)' - f''u - f' - (\log \rho)' = 0. \quad (20)$$

Proof. In 1-dimensional case, the equation (3) follows

$$\nabla^2(\rho \nabla^2 \Phi) - \nabla(\rho \nabla^2 f \nabla \Phi) - \nabla(\rho \nabla f) - \nabla^2 \rho = 0.$$

The above equation is equivalent to

$$\rho \nabla^3 \Phi + \nabla \rho \nabla^2 \Phi - \rho \nabla^2 f \nabla \Phi - \rho \nabla f - \nabla \rho + C = 0,$$

where C is a constant. Because $\rho \in \mathcal{P}(\mathbb{R}) \subset L^1(\mathbb{R})$. Hence $\lim_{|x| \rightarrow \infty} \rho(x) = 0$, which indicates $C = 0$. Suppose that $\rho > 0$ and let $u = \nabla \Phi$. Dividing both sides by ρ , we obtain

$$u'' + u' \rho' / \rho - f''u - f' - \rho' / \rho = 0.$$

By the fact that $\rho' / \rho = (\log \rho)'$, we derive (20). \square

We consider the case where $f'(x)$ and $(\log \rho)'(x)$ are affine functions. Then, ODE (20) has a closed-form solution. Applying ODE (20), we present the exact formulation of Newton's Langevin dynamics.

Proposition 7. *Assume that $f(x) = (2\Sigma^*)^{-1}(x - \mu^*)^2$, where $\Sigma^* > 0$ and μ^* are given. Suppose that the particle system X_0 follows the Gaussian distribution. Then X_t follows a Gaussian distribution with mean μ_t and variance Σ_t . The corresponding NLD satisfies*

$$dX_t = \left(\frac{\Sigma^* - \Sigma}{\Sigma^* + \Sigma_t} X_t - \frac{2\Sigma^*}{\Sigma^* + \Sigma_t} \mu_t + \mu^* \right) dt.$$

And the evolution of μ_t and Σ_t satisfies

$$d\mu_t = (-\mu_t + \mu^*)dt, \quad d\Sigma_t = 2\frac{\Sigma^* - \Sigma_t}{\Sigma^* + \Sigma_t}\Sigma_t dt.$$

The explicit solutions of μ_t and Σ_t satisfy

$$\mu_t = e^{-t}(\mu_0 - \mu^*) + \mu^*, \quad \Sigma_t = \Sigma^* + (\Sigma_0 - \Sigma^*)e^{-t}\sqrt{\frac{e^{-2t}(\Sigma_0 - \Sigma^*)^2}{4\Sigma_0^2} + \frac{1}{\Sigma_0\Sigma^*}}.$$

Proof. In section 5 Proposition 10, we show that if the evolution of X_t follows NLD, then X_t follows the Gaussian distribution. We first solve the Newton's direction from ODE (20). Suppose that $(\log \rho)'(x) = \Sigma^{-1}(x - \mu)$. The ODE turns to be

$$u'' - u'\Sigma^{-1}(x - \mu) - (\Sigma^*)^{-1}u - (\Sigma^*)^{-1}(x - \mu^*) + \Sigma^{-1}(x - \mu) = 0.$$

We can examine that the following u is a solution to the above ODE.

$$u(x) = \frac{\Sigma^{-1} - (\Sigma^*)^{-1}}{\Sigma^{-1} + (\Sigma^*)^{-1}}x - \frac{2\Sigma^{-1}}{\Sigma^{-1} + (\Sigma^*)^{-1}}\mu + \mu^*.$$

Hence, we have $\Phi^{\text{Newton}}(x) = \frac{\Sigma^* - \Sigma}{2(\Sigma^* + \Sigma)}x^2 - \frac{2\Sigma^*}{\Sigma^* + \Sigma}\mu x + \mu^*x$. As a result, NLD follows

$$dX_t = \left(\frac{\Sigma^* - \Sigma_t}{\Sigma^* + \Sigma_t}X_t - \frac{2\Sigma^*}{\Sigma^* + \Sigma_t}\mu_t + \mu^* \right) dt.$$

The dynamics of μ_t satisfies

$$d\mu_t = d\mathbb{E}[X_t] = \mathbb{E}[dX_t] = \left(\frac{\Sigma^* - \Sigma_t}{\Sigma^* + \Sigma_t}\mu_t - \frac{2\Sigma^*}{\Sigma^* + \Sigma_t}\mu_t + \mu^* \right) dt = (-\mu_t + \mu^*)dt.$$

This indicates that $\mu_t = \mu^* + e^{-t}(\mu_0 - \mu^*)$. The dynamics of Σ_t follows

$$\begin{aligned} d\Sigma_t &= d(\mathbb{E}[X_t^2] - \mu_t^2) = 2\mathbb{E}[X_t dX_t] - 2\mu_t d\mu_t \\ &= 2 \left[\frac{\Sigma^* - \Sigma_t}{\Sigma^* + \Sigma_t} (\Sigma_t + \mu_t^2) - \frac{2\Sigma^*}{\Sigma^* + \Sigma_t} \mu_t^2 + \mu^* \mu_t - \mu_t(-\mu_t + \mu^*) \right] dt = 2\frac{\Sigma^* - \Sigma_t}{\Sigma^* + \Sigma_t}\Sigma_t dt. \end{aligned}$$

We can rewrite that

$$dt = \frac{(\Sigma^* + \Sigma_t)d\Sigma_t}{2(\Sigma^* - \Sigma_t)\Sigma_t} = \left(\frac{1}{(\Sigma^* - \Sigma_t)} + \frac{1}{2\Sigma_t} \right) d\Sigma_t.$$

Integrating both sides of the above equation yields

$$t - \log |\Sigma^* - \Sigma_0| + \frac{1}{2} \log \Sigma_0 = -\log |\Sigma^* - \Sigma_t| + \frac{1}{2} \log \Sigma_t, \quad (\Sigma_t - \Sigma^*)^2 = \frac{(\Sigma_0 - \Sigma^*)^2}{\Sigma_0} e^{-2t\Sigma_t}.$$

Hence, the solution Σ_t follows

$$\Sigma_t = \Sigma^* + \frac{e^{-2t}(\Sigma_0 - \Sigma^*)^2}{2\Sigma_0} + (\Sigma_0 - \Sigma^*)e^{-t}\sqrt{\frac{e^{-2t}(\Sigma_0 - \Sigma^*)^2}{4\Sigma_0^2} + \frac{\Sigma^*}{\Sigma_0}}.$$

□

Now, we are ready to compare the NLD with OLD, LLD and HAMCMC. Here we consider $f(x) = (2\Sigma^*)^{-1}(x - \mu^*)^2$, where $\Sigma^* > 0$ and μ^* are given. The OLD satisfies

$$dX_t = -(\Sigma^*)^{-1}(X_t - \mu^*)dt + \sqrt{2}dB_t,$$

which is also known as the Ornstein-Uhlenbeck process. And LLD writes

$$dX_t = -(\Sigma^*)^{-1}(X_t - \mu^*)dt + \Sigma_t^{-1}(X_t - \mu_t)dt.$$

The mean μ_t and variance Σ_t of OLD and LLD both satisfy

$$\mu_t = \mu^* + e^{-(\Sigma^*)^{-1}t}(\mu_0 - \mu^*), \quad \Sigma_t = \Sigma^* + e^{-2(\Sigma^*)^{-1}t}(\Sigma_0 - \Sigma^*).$$

On the other hand, HAMCMC follows the dynamics

$$dX_t = -(X_t - \mu^*)dt + \sqrt{2\Sigma^*}dB_t.$$

For HAMCMC, the evolution of mean μ_t follows

$$d\mu_t = d\mathbb{E}[X_t] = -(\mu_t - \mu^*)dt,$$

and the evolution of variance Σ_t satisfies

$$\begin{aligned} d\Sigma_t &= d(\mathbb{E}[X_t^2] - \mu_t^2) = 2\mathbb{E}[X_t dX_t] - 2\mu_t d\mu_t \\ &= 2 \left[-(\Sigma_t + \mu_t^2) + \mu^* \mu_t + \Sigma^* + \mu_t(\mu_t - \mu^*) \right] dt = 2(\Sigma^* - \Sigma_t)dt. \end{aligned}$$

The mean μ_t and variance Σ_t of HAMCMC follows

$$\mu_t = \mu^* + e^{-t}(\mu_0 - \mu^*), \quad \Sigma_t = \Sigma^* + e^{-2t}(\Sigma_0 - \Sigma^*).$$

We summarized our results in Table 1.

Dynamics	Particle	Mean and variance
NLD	$dX_t = \left(\frac{\Sigma^* - \Sigma_t}{\Sigma^* + \Sigma_t} X_t - \frac{2\Sigma^*}{\Sigma^* + \Sigma_t} \mu_t + \mu^* \right) dt$	$\mu_t = \mu^* + e^{-t}(\mu_0 - \mu^*)$ $\frac{\Sigma_t - \Sigma^*}{\Sigma_0 - \Sigma^*} = \frac{e^{-2t}(\Sigma_0 - \Sigma^*)}{2\Sigma_0}$ $+ e^{-t} \sqrt{\frac{e^{-2t}(\Sigma_0 - \Sigma^*)^2}{4\Sigma_0^2} + \frac{\Sigma^*}{\Sigma_0}}$
OLD	$dX_t = -(\Sigma^*)^{-1}(X_t - \mu^*)dt + \sqrt{2}dB_t$	$\mu_t = \mu^* + e^{-(\Sigma^*)^{-1}t}(\mu_0 - \mu^*)$
LLD	$dX_t = -(\Sigma^*)^{-1}(X_t - \mu^*)dt + \Sigma_t^{-1}(X_t - \mu_t)dt$	$\Sigma_t = \Sigma^* + e^{-2(\Sigma^*)^{-1}t}(\Sigma_0 - \Sigma^*)$
HAMCMC	$dX_t = -(X_t - \mu^*)dt + \sqrt{2\Sigma^*}dB_t.$	$\mu_t = \mu^* + e^{-t}(\mu_0 - \mu^*)$ $\Sigma_t = \Sigma^* + e^{-2t}(\Sigma_0 - \Sigma^*)$

TABLE 1. Comparison among different Langevin dynamics on 1D Gaussian family.

Compared to OLD and LLD, the exponential convergence rate of μ_t and Σ_t in NLD does not depend on Σ^* . This fact shows that the NLD is the Newton's flow for both the evolution of mean and variance in Gaussian process. We also note that the convergence rates of mean and variance are different in HAMCMC, while they are same in NLD. Later on in section 8, we use numerical examples to further demonstrate the differences between NLD and HAMCMC.

5. NEWTON'S FLOWS IN GAUSSIAN FAMILIES

In this section, we study information Newton's flows in Gaussian families with respect to Wasserstein metric. Let \mathbb{P}^n and \mathbb{S}^n represent the space of symmetric positive definite matrices and symmetric matrices with size $n \times n$ respectively.

We let \mathcal{N}_n^0 denote multivariate Gaussian densities with zero means. Each $\rho \in \mathcal{N}_n^0$ is uniquely determined by its covariance matrix $\Sigma \in \mathbb{P}^n$. So we can view $\mathcal{N}_n^0 \simeq \mathbb{P}^n$. The Wasserstein metric $\mathcal{G}^W(\rho)$ on $\mathcal{P}(\mathbb{R}^n)$ induces the Wasserstein metric $\mathcal{G}^W(\Sigma)$ on \mathbb{P}^n ,

see (Takatsu, 2008; Modin, 2016; Malagò et al., 2018). For $\Sigma \in \mathbb{P}^n$, tangent space and cotangent space follow

$$T_\Sigma \mathbb{P}^n \simeq T_\Sigma^* \mathbb{P}^n \simeq \mathbb{S}^n.$$

Definition 4 (Wasserstein metric in Gaussian families). *Given $\Sigma \in \mathbb{P}^n$, the Wasserstein metric tensor $\mathcal{G}^W(\Sigma) : \mathbb{S}^n \rightarrow \mathbb{S}^n$ is defined by*

$$\mathcal{G}^W(\Sigma)^{-1}S = 2(\Sigma S + S\Sigma).$$

It defines an inner product on the tangent space $T_\Sigma \mathbb{P}^n$. Namely, for $A_1, A_2 \in T_\Sigma \mathbb{P}^n \simeq \mathbb{S}^n$

$$g_\Sigma^W(A_1, A_2) = \text{tr}(A_1 \mathcal{G}^W(\Sigma) A_2) = \text{tr}(S_1 \mathcal{G}^W(\Sigma)^{-1} S_2) = 4 \text{tr}(S_1 \Sigma S_2).$$

Here $S_i \in T_\Sigma^ \mathbb{P}^n \simeq \mathbb{S}^n$ is the solution to discrete Lyapunov equation*

$$A_i = 2(\Sigma S_i + S_i \Sigma), \quad i = 1, 2.$$

For $\Sigma \in \mathbb{P}^n$, there exists a unique solution to discrete Lyapunov equation. Again, we focus on the case where the objective functional $E(\Sigma)$ evaluates the KL divergence from ρ with covariance matrix Σ to a target Gaussian density ρ^* with covariance matrix Σ^* . Then, $E(\Sigma)$ satisfies

$$E(\Sigma) = \frac{1}{2} (\text{tr}(\Sigma(\Sigma^*)^{-1}) - n - \log \det(\Sigma(\Sigma^*)^{-1})). \quad (21)$$

Proposition 8 (Gradient and Hessian operators in \mathbb{P}^n). *The gradient operator follows*

$$\text{grad}^W E(\Sigma) = \mathcal{G}^W(\Sigma)^{-1} \nabla E(\Sigma) = \Sigma(\Sigma^*)^{-1} + (\Sigma^*)^{-1} \Sigma - 2I.$$

And the Hessian operator satisfies that for all $A \in \mathbb{S}^n$,

$$g_\Sigma^W(A, \text{Hess}^W E(\Sigma) A) = 4 \text{tr}(S \Sigma S (\Sigma^*)^{-1}) + 4 \text{tr}(S^2),$$

where S is the unique solution to $A = 2(\Sigma S + S\Sigma)$.

Proof. Given $A \in \mathbb{S}^n$, the geodesic curve $\hat{\Sigma}_s$ with $\hat{\Sigma}_s|_{s=0} = \Sigma$ and $\partial_s \hat{\Sigma}_s|_{s=0} = A$ follows $\hat{\Sigma}_s = (I + 2sS)\Sigma(I + 2sS)$, where $S = \mathcal{G}(\Sigma)^{-1}A$ is the solution to $A = 2(\Sigma S + S\Sigma)$. We can compute that

$$E(\hat{\Sigma}_s) = \frac{1}{2} (\text{tr}((I + 2sS)\Sigma(I + 2sS)(\Sigma^*)^{-1}) - n - \log \det((I + 2sS)\Sigma(I + 2sS)(\Sigma^*)^{-1})).$$

The Taylor expansion of $\log \det(I + sS)$ w.r.t. s satisfies

$$\log \det(I + sS) = s \text{tr}(S) - \frac{s^2}{2} \text{tr}(S^2) + o(s^2).$$

Hence, the first-order derivative follows

$$\begin{aligned} \left. \frac{\partial}{\partial s} E(\Sigma(s)) \right|_{s=0} &= \text{tr}(S \Sigma (\Sigma^*)^{-1}) + \text{tr}(\Sigma S (\Sigma^*)^{-1}) - 2 \text{tr}(S) \\ &= \text{tr}(S (\Sigma (\Sigma^*)^{-1} + (\Sigma^*)^{-1} \Sigma - 2I)). \end{aligned}$$

By the definition $\left. \frac{\partial}{\partial s} E(\Sigma(s)) \right|_{s=0} = \text{tr}(S \text{grad} E(\Sigma))$, this yields $\text{grad} E(\Sigma) = \Sigma(\Sigma^*)^{-1} + (\Sigma^*)^{-1} \Sigma - 2I$ and the second-order derivative follows

$$\left. \frac{\partial^2}{\partial s^2} E(\Sigma(s)) \right|_{s=0} = 4 \text{tr}(S \Sigma S (\Sigma^*)^{-1}) + 4 \text{tr}(S^2).$$

This completes the proof. \square

Similarly, let us consider the linear self-adjoint operator $\mathcal{H}_E^W(\Sigma) : \mathbb{S}^n \rightarrow \mathbb{S}^n$, which defines a bi-linear form

$$\text{tr}(S\mathcal{H}_E^W(\Sigma)S) = g_\Sigma^W(A, \text{Hess}^W E(\Sigma)A) = 4 \text{tr}(S\Sigma S(\Sigma^*)^{-1}) + 4 \text{tr}(S^2).$$

We can compute that $\mathcal{H}_E(\Sigma)$ is uniquely defined by

$$\mathcal{H}_E(\Sigma)S = 2\Sigma S(\Sigma^*)^{-1} + 2(\Sigma^*)^{-1}S\Sigma + 4S, \quad \forall S \in \mathbb{S}^n.$$

Because $\text{tr}(S\mathcal{H}_E(\Sigma)S) = 4 \text{tr}(S\Sigma S(\Sigma^*)^{-1}) + 4 \text{tr}(S^2) > 0$ for $S \neq 0, S \in \mathbb{S}^n$, \mathcal{H}_E is injective and invertible. Now, we are ready to present the Newton's flow of KL divergence in Gaussian families.

Proposition 9. *The Newton's flow of KL divergence in Gaussian families follows*

$$\begin{cases} \dot{\Sigma}_t - 2(S\Sigma_t + \Sigma S_t) = 0, \\ 2\Sigma_t S_t (\Sigma^*)^{-1} + 2(\Sigma^*)^{-1} S_t \Sigma_t + 4S_t = -(\Sigma_t (\Sigma^*)^{-1} + (\Sigma^*)^{-1} \Sigma_t - 2I). \end{cases} \quad (22)$$

Proof. The Newton's flow follows

$$\dot{\Sigma}_t - (\text{Hess}^W E(\Sigma_t))^{-1} \text{grad}^W E(\Sigma_t) = 0.$$

We note that $\text{Hess}^W E(\Sigma)\mathcal{G}^W(\Sigma)^{-1} = \mathcal{H}_E^W(\Sigma)$, which implies

$$(\text{Hess}^W E(\Sigma))^{-1} = \mathcal{G}^W(\Sigma)^{-1} \mathcal{H}_E^W(\Sigma)^{-1}.$$

Hence, we can reformulate the Newton's flow by

$$\begin{cases} \dot{\Sigma}_t - \mathcal{G}^W(\Sigma_t)^{-1} S_t = 0, \\ \mathcal{H}_E^W(\Sigma_t) S_t = -\text{grad}^W E(\Sigma_t). \end{cases}$$

From the formulations of $\mathcal{G}(\Sigma)^{-1}$, $\text{grad}^W E(\Sigma)$ and $\mathcal{H}_E(\Sigma)$, we obtain (22). \square

Example 12. *In one dimensional case, the second equation in (22) has an explicit solution $S_t = -\frac{(\Sigma^*)^{-1}\Sigma_t - 1}{2((\Sigma^*)^{-1}\Sigma_t + 1)}$. Let $\Sigma_t = Y_t^2$, where $Y_t > 0$. Then, the first equation in (22) turns to*

$$2Y_t \dot{Y}_t + 4Y_t^2 \frac{(\Sigma^*)^{-1}Y_t^2 - 1}{2((\Sigma^*)^{-1}Y_t^2 + 1)} = 0,$$

or equivalently,

$$\dot{Y}_t + \frac{(\Sigma^*)^{-1}Y_t - Y_t^{-1}}{(\Sigma^*)^{-1} + Y_t^{-2}} = 0. \quad (23)$$

Let $f(Y) = \frac{1}{2}((\Sigma^*)^{-1}Y^2 - 1 - \log((\Sigma^*)^{-1}Y^2))$. Then, we have $\nabla f(Y) = (\Sigma^*)^{-1}Y - Y^{-1}$ and $\nabla^2 f(Y) = (\Sigma^*)^{-1} + Y^{-2}$. Hence, the Newton's flow (23) coincides with Newton's flow of $f(X)$ in Euclidean space. We also note that (23) is identical to the evolution of Σ_t in Proposition 7 by substituting $\Sigma_t = Y_t^2$.

Proposition 10 ensures the existence of information Newton's flows in Gaussian families.

Proposition 10. *Suppose that $\rho^0, \rho^* \in \mathcal{N}_0^n$ and their covariance matrices are Σ^0 and Σ^* . $E(\Sigma)$ defined in (21) evaluates the KL divergence from ρ to ρ^* . Let (Σ_t, S_t) satisfy (22) with initial values $\Sigma_t|_{t=0} = \Sigma^0$ and $S_t|_{t=0} = 0$. Thus, for any $t \geq 0$, Σ_t is well-defined and stays positive definite. Consider*

$$\rho_t(x) = \frac{(2\pi)^{-n/2}}{\sqrt{\det(\Sigma_t)}} \exp\left(-\frac{1}{2}x^T \Sigma_t^{-1}x\right), \quad \Phi_t(x) = x^T S_t x + C(t),$$

where $C(t) = -t + \frac{1}{2} \int_0^t \log \det(\Sigma_s(\Sigma^*)^{-1}) ds$. Then, ρ_t and Φ_t follow the information Newton's flow (3) with initial values $\rho_t|_{t=0} = \rho^0$ and $\Phi_t|_{t=0} = 0$.

Proof. We first prove that Σ_t is positive definite. We formulate that

$$\begin{aligned} \partial_t E(\Sigma_t) &= \text{tr}(\partial_t \Sigma_t \nabla E(\Sigma_t)) = 2 \text{tr}(S_t \Sigma_t ((\Sigma^*)^{-1} - \Sigma_t^{-1})) \\ &= \text{tr}(S_t (\Sigma_t (\Sigma^*)^{-1} + (\Sigma^*)^{-1} \Sigma_t - 2I)) = -\text{tr}(S(2\Sigma S_t (\Sigma^*)^{-1} + 2(\Sigma^*)^{-1} S_t \Sigma_t + 4S_t)) \\ &= -4 \text{tr}(S_t \Sigma_t S_t (\Sigma^*)^{-1}) - 4 \text{tr}(S_t^2) \leq 0. \end{aligned}$$

As a result, $E(\Sigma_t)$ is non-increasing. Applying the idea of proof in (Wang and Li, 2019, Theorem 1), we can establish that Σ_t is positive definite. Then, we examine that Φ_t satisfies (3). We observe that

$$\begin{aligned} \nabla^2 : (\rho_t \nabla^2 \Phi_t) - \nabla \cdot (\rho_t \nabla^2 f \nabla \Phi_t) - \nabla \cdot (\rho_t \nabla f) - \Delta \rho_t \\ = 2\nabla^2 : (S_t \rho_t(x)) - 2\nabla \cdot (\rho_t(x) (\Sigma^*)^{-1} S_t x) - \nabla \cdot (\rho_t(x) (\Sigma^*)^{-1} x) - \Delta \rho_t. \end{aligned}$$

We note that $\nabla \rho_t(x) = -\Sigma_t^{-1} x \rho_t(x)$ and $\nabla^2 \rho_t(x) = -\Sigma_t^{-1} \rho_t(x) + \Sigma_t^{-1} x x^T \Sigma_t^{-1} \rho_t(x)$. Hence, we derive all four terms in the above equation as follows. First, it is easy to observe that

$$\nabla^2 : (\rho_t(x) S_t) = \text{tr}(S_t \nabla^2 \rho_t(x)), \quad -\Delta \rho_t = -\nabla^2 : (\rho_t I) = -\text{tr}(\nabla^2 \rho_t(x)).$$

We can also compute that

$$\begin{aligned} & -\nabla \cdot (\rho_t (\Sigma^*)^{-1} S_t x) \\ &= -\sum_{i=1}^n \partial_i (\rho_t(x) W S_t x)_i \\ &= -\sum_{i=1}^n [\rho_t(x) \partial_i ((\Sigma^*)^{-1} S_t x)_i + (W S_t x)_i \partial_i \rho_t(x)] \\ &= -\rho_t(x) [\text{tr}((\Sigma^*)^{-1} S_t) + ((\Sigma^*)^{-1} S_t x)^T (-\Sigma_t^{-1} x)] \\ &= -\rho_t(x) \text{tr}(S_t (\Sigma^*)^{-1} (I - \Sigma_t^{-1} x x^T)) \\ &= \frac{1}{2} \text{tr}((\Sigma_t S_t (\Sigma^*)^{-1} + (\Sigma^*)^{-1} S_t \Sigma_t) \nabla^2 \rho_t(x)). \end{aligned}$$

Taking $S_t = I$ into the above equation yields

$$-\nabla \cdot (\rho_t (\Sigma^*)^{-1} x) = \frac{1}{2} \text{tr}((\Sigma_t (\Sigma^*)^{-1} + (\Sigma^*)^{-1} \Sigma_t) \nabla^2 \rho_t(x)).$$

Because (Σ_t, S_t) satisfies (22), we have

$$\begin{aligned} & 2\nabla^2 : (S_t \rho_t(x)) - 2\nabla \cdot (\rho_t(x) (\Sigma^*)^{-1} S_t x) - \nabla \cdot (\rho_t(x) (\Sigma^*)^{-1} x) - \Delta \rho_t \\ &= \text{tr}((2S_t + \Sigma_t S_t (\Sigma^*)^{-1} + (\Sigma^*)^{-1} S_t \Sigma_t + \Sigma_t (\Sigma^*)^{-1} + (\Sigma^*)^{-1} \Sigma_t - 2I) \nabla^2 \rho_t(x)) \\ &= 0. \end{aligned}$$

This completes the proof. \square

Remark 5. Proposition 10 also indicates the fact that if the evolution of X_t follows NLD, then X_t follows the Gaussian distribution.

6. INFORMATION NEWTON'S METHOD AND CONVERGENCE ANALYSIS

In this section, we introduce a general update rule of information Newton's method for probability densities and analyze its convergence rate.

The general update rule of the Newton's method follows

$$\rho_{k+1} = \text{Exp}_{\rho_k}^{\alpha_k}(\Phi_k), \quad \mathcal{H}_E(\rho_k)\Phi_k + \mathcal{G}(\rho_k)^{-1} \frac{\delta E}{\delta \rho_k} = 0. \quad (24)$$

Here $\alpha_k > 0$ is a step size. Here $\text{Exp}_{\rho_k}^{\alpha_k}(\Phi_k)$ is the exponential map, which we elaborate in subsection 6.1.

6.1. Riemannian structure of probability space. We first provide some background knowledge for the Riemannian structure of probability space. Given a metric tensor $\mathcal{G}(\rho)$ and two probability densities $\rho_0, \rho_1 \in \mathcal{P}(\Omega)$, we define the distance $\mathcal{D}(\rho_0, \rho_1)$ as follows

$$\mathcal{D}(\rho_0, \rho_1)^2 = \inf_{\hat{\rho}_s, s \in [0,1]} \left\{ \int_0^1 \int \partial_s \hat{\rho}_s \mathcal{G}(\hat{\rho}_s)^{-1} \partial_s \hat{\rho}_s dx ds : \hat{\rho}_s|_{s=0} = \rho_0, \hat{\rho}_s|_{s=1} = \rho_1 \right\}.$$

The minimizer $\hat{\rho}_s$ is the geodesic curve (6) connecting ρ_0 and ρ_1 . For the Wasserstein metric $\mathcal{G}(\rho) = \mathcal{G}^W(\rho)$, $\mathcal{D}(\rho_0, \rho_1)$ is the Wasserstein-2 distance between ρ_0 and ρ_1 .

For simplicity, we define the exponential map and other Riemannian operators on cotangent space.

Definition 5 (Exponential map on cotangent space and its inverse). *The exponential map Exp_{ρ_0} is a mapping from the cotangent space $T_{\rho_0}^* \mathcal{P}(\Omega)$ to $\mathcal{P}(\Omega)$. Namely, $\text{Exp}_{\rho_0}(\Phi) = \hat{\rho}_s|_{s=1}$. Here $\hat{\rho}_s, s \in [0, 1]$ is the solution to geodesic equation (6) with initial conditions $\hat{\rho}_s|_{s=0} = \rho_0, \Phi_s|_{s=0} = \Phi$.*

The inverse of the exponential map $\text{Exp}_{\rho_0}(\rho_1)$ follows $\text{Exp}_{\rho_0}^{-1}(\rho_1) = \mathcal{G}(\hat{\rho}_s)\partial_s \hat{\rho}_s|_{s=0}$. Here $\hat{\rho}_s, s \in [0, 1]$ is the solution to geodesic equation (6) with boundary conditions $\hat{\rho}_s|_{s=0} = \rho_0$ and $\hat{\rho}_s|_{s=1} = \rho_1$.

For simplicity, we denote the inner product on cotangent space $T_{\rho}^* \mathcal{P}(\Omega)$ by

$$\langle \Phi_1, \Phi_2 \rangle_{\rho} = \int \Phi_1 \mathcal{G}(\rho)^{-1} \Phi_2 dx, \quad \Phi_1, \Phi_2 \in T_{\rho}^* \mathcal{P}(\Omega),$$

and $\|\Phi\|_{\rho}^2 = \langle \Phi, \Phi \rangle_{\rho}$. We also denote $\text{Exp}_{\rho}^{\alpha}(\Phi)$ to be the solution at time $t = \alpha$ to the geodesic equation (6) with initial values $\hat{\rho}_0 = \rho$ and $\Phi_0 = \Phi$. As a known result of Riemannian geometry, the geodesic curve has constant speed (Boothby, 1986). Namely, for $\Phi \in T_{\rho}^* \mathcal{P}(\Omega)$ and $\alpha > 0$, we have

$$\text{Exp}_{\rho}^{\alpha}(\Phi) = \text{Exp}_{\rho}(\alpha \Phi).$$

And for $\rho_0, \rho_1 \in \mathcal{P}(\Omega)$, it follows

$$\|\text{Exp}_{\rho_0}^{-1}(\rho_1)\|_{\rho_0}^2 = \mathcal{D}(\rho_0, \rho_1)^2.$$

To prove the convergence rate, we introduce the definition of the parallelism.

Definition 6 (Parallelism). *Suppose that $\bar{\rho}_s$ is the geodesic curve connecting ρ^0 and ρ^1 . We say that $\tau : T_{\rho^0} \mathcal{P}(\Omega) \rightarrow T_{\rho^1} \mathcal{P}(\Omega)$ is a parallelism from ρ^0 to ρ^1 , if for all $\Phi_1, \Phi_2 \in T_{\rho^0} \mathcal{P}(\Omega)$, it follows*

$$\langle \Phi_1, \Phi_2 \rangle_{\rho^0} = \langle \tau \Phi_1, \tau \Phi_2 \rangle_{\rho^1}.$$

We define high-order derivatives on the cotangent-space in Proposition 11.

Proposition 11. *For all $\Phi \in T_\rho^*\mathcal{P}(\Omega)$, it follows*

$$\begin{aligned} E(\text{Exp}_\rho^s(\Phi)) &= E(\rho) + s\nabla E(\rho)(\Phi) + \dots + \frac{s^{n-1}}{(n-1)!} \nabla^{n-1} E(\rho)(\Phi, \dots, \Phi) \\ &\quad + \frac{s^n}{n!} \nabla^n E(\text{Exp}_\rho^\lambda(\Phi))(\tau_\lambda \Phi, \dots, \tau_\lambda \Phi), \end{aligned}$$

where τ_λ is the parallelism from ρ to $\text{Exp}_\rho^\lambda(\Phi)$ and $\lambda \in (0, s)$. Here $\nabla^n E(\rho)$ defines a n -form on the cotangent space $T_\rho^*\mathcal{P}(\Omega)$. Namely, it is recursively defined by

$$\nabla^n E(\rho)(\Phi_1, \dots, \Phi_n) = \left. \frac{\partial}{\partial s} \nabla^{n-1} E(\text{Exp}_\rho^s(\Phi_n))(\tau_s \Phi_1, \dots, \tau_s \Phi_{n-1}) \right|_{s=0},$$

where τ_s is the parallelism from ρ to $\text{Exp}_\rho^s(\Phi_n)$.

Proof. We first show that

$$\frac{\partial}{\partial s} \nabla^{n-1} E(\text{Exp}_\rho^s(\Phi_n))(\tau_s \Phi_1, \dots, \tau_s \Phi_{n-1}) = \nabla^n E(\text{Exp}_\rho^s(\Phi_n))(\tau_s \Phi_1, \dots, \tau_s \Phi_n). \quad (25)$$

From the definition, it follows that

$$\begin{aligned} & \frac{\partial}{\partial s} \nabla^{n-1} E(\text{Exp}_\rho^s(\Phi_n))(\tau_s \Phi_1, \dots, \tau_s \Phi_{n-1}) \\ &= \left. \frac{\partial}{\partial t} \nabla^{n-1} E(\text{Exp}_\rho^{s+t}(\Phi_n))(\tau_{s+t} \Phi_1, \dots, \tau_{s+t} \Phi_{n-1}) \right|_{t=0} \\ &= \left. \frac{\partial}{\partial t} \nabla^{n-1} E(\text{Exp}_{\text{Exp}_\rho^s(\Phi_n)}^t(\tau_s \Phi_n))(\tau_t \tau_s \Phi_1, \dots, \tau_t \tau_s \Phi_{n-1}) \right|_{t=0} \\ &= \nabla^n E(\text{Exp}_\rho^s(\Phi_n))(\tau_s \Phi_1, \dots, \tau_s \Phi_n). \end{aligned}$$

From (25), we can recursively compute that

$$\frac{\partial^n}{(\partial s)^n} E(\text{Exp}_\rho^s(\Phi)) = \nabla^n E(\text{Exp}_\rho^s(\Phi))(\tau_s \Phi, \dots, \tau_s \Phi).$$

The Taylor expansion of $E(\text{Exp}_\rho^s(\Phi))$ w.r.t. s completes the proof. \square

Remark 6. *For the first-order derivative of $E(\rho)$, it follows*

$$\nabla E(\rho)(\Phi) = \int \Phi \mathcal{G}(\rho)^{-1} \frac{\delta E}{\delta \rho} dx.$$

For the second-order derivative of $E(\rho)$, it satisfies

$$\nabla^2 E(\rho)(\Phi_1, \Phi_2) = \int \Phi_1 \mathcal{H}_E(\rho) \Phi_2 dx.$$

6.2. Convergence analysis. To ensure the convergence of Newton's method in Euclidean space, it is assumed that $\nabla^2 f(x)$ is positive definite around a small neighbour of the optimal solution x^* . To prove the convergence rate of Newton's method in the probability space, we assume the following fact analogously.

Assumption 1. Assume that there exists $\epsilon > 0$, such that for all ρ satisfying $\mathcal{D}(\rho, \rho^*) < \epsilon$, it follows

$$\begin{aligned} |\nabla^2 E(\rho)(\Phi_1, \Phi_1)| &\geq \delta_1 \|\Phi_1\|_\rho^2, \\ |\nabla^2 E(\rho)(\Phi_1, \Phi_1)| &\leq \delta_2 \|\Phi_1\|_\rho^2, \\ |\nabla^3 E(\rho)(\Phi_1, \Phi_1, \Phi_2)| &\leq \delta_3 \|\Phi_1\|_\rho^2 \|\Phi_2\|_\rho, \end{aligned}$$

holds for all $\Phi_1, \Phi_2 \in T_\rho^* \mathcal{P}(\Omega)$.

Relying on Assumption 1, Theorem 3 shows the quadratic convergence rate of the Newton's method in the probability space.

Theorem 3. Suppose that Assumption 1 holds, ρ_k satisfies $\mathcal{D}(\rho_k, \rho^*) < \epsilon$ and the step size $\tau_k = 1$. Then, we have

$$\mathcal{D}(\rho_{k+1}, \rho^*) = O(\mathcal{D}(\rho_k, \rho^*)^2),$$

Here we follow the proof technique in (Smith, 1994, Section 4, Theorem 4.4). We begin with Lemma 3.

Lemma 3 (Cauchy-Schwarz inequality). Suppose that $\mathcal{H} : T_\rho^* \mathcal{P}(\Omega) \rightarrow T_\rho \mathcal{P}(\Omega)$ is a self-adjoint linear operator and \mathcal{H} is positive definite. Then, for $\Phi_1, \Phi_2 \in T_\rho^* \mathcal{P}(\Omega)$, we have

$$\left(\int \Phi_1 \mathcal{H} \Phi_2 dx \right)^2 \leq \left(\int \Phi_1 \mathcal{H} \Phi_1 dx \right) \left(\int \Phi_2 \mathcal{H} \Phi_2 dx \right).$$

Proof. The proof is quite similar to the Euclidean space. For all $s \in \mathbb{R}$, we have

$$\begin{aligned} 0 &\leq \int (\Phi_1 + s\Phi_2) \mathcal{H} (\Phi_1 + s\Phi_2) dx \\ &= s^2 \int \Phi_2 \mathcal{H} \Phi_2 dx + 2s \int \Phi_1 \mathcal{H} \Phi_2 dx + \int \Phi_1 \mathcal{H} \Phi_1 dx. \end{aligned}$$

Because the arbitrary choice of s , it follows that

$$\left(2 \int \Phi_1 \mathcal{H} (\rho) \Phi_2 dx \right)^2 - 4 \left(\int \Phi_1 \mathcal{H} (\rho) \Phi_1 dx \right) \left(\int \Phi_2 \mathcal{H} (\rho) \Phi_2 dx \right) \geq 0.$$

This completes the proof. \square

For simplicity, we denote $T_k = \text{Exp}_{\rho_k}^{-1}(\rho^*)$.

Lemma 4. For all $\Phi \in T_{\rho_k}^* \mathcal{P}(\Omega)$, it follows

$$\nabla E(\rho_k)(\Phi) + \nabla^2 E(\rho_k)(T_k, \Phi) = -\frac{1}{2} \nabla^3 E(\text{Exp}_{\rho_k}^\lambda)(\tau_\lambda T_k, \tau_\lambda T_k, \tau_\lambda \Phi),$$

where τ_λ is the parallelism from ρ_k to $\text{Exp}_{\rho_k}^\lambda(T_k)$ and $\lambda \in (0, 1)$.

Proof. Consider the auxiliary function

$$A(s) = \nabla E(\text{Exp}_{\rho_k}^s(T_k))(\tau_s \Phi).$$

Directly from the definition of high-order derivatives, it follows

$$\frac{\partial}{\partial s} A(s) = \nabla^2 E(\text{Exp}_{\rho_k}^s(T_k))(\tau_s T_k, \tau_s \Phi),$$

$$\frac{\partial^2}{\partial s^2} A(s) = \nabla^3 E(\text{Exp}_{\rho_k}^s(T_k))(\tau_s T_k, \tau_s T_k, \tau_s \Phi).$$

Hence, we can compute the Taylor expansion

$$\nabla E(\text{Exp}_{\rho_k}^1(T_k))(\tau_1 \Phi) = \nabla E(\rho_k)(\Phi) + \nabla^2 E(\rho_k)(T_k, \Phi) + \frac{1}{2} \nabla^3 E(\text{Exp}_{\rho_k}^\lambda)(\tau_\lambda T_k, \tau_\lambda T_k, \tau_\lambda \Phi).$$

On the other hand, we notice that

$$\nabla E(\text{Exp}_{\rho_k}^1(T_k))(\tau_1 \Phi) = \nabla E(\rho^*)(\tau_1 \Phi) = \int \tau_1 \Phi \mathcal{G}(\rho)^{-1} \frac{\delta E}{\delta \rho^*} dx = 0.$$

This completes the proof. \square

Let τ be the parallelism from ρ_k to ρ_{k+1} . There exists a unique $R_k \in T_{\rho_k}^* \mathcal{P}(\Omega)$ such that

$$T_k = \tau^{-1} T_{k+1} + \Phi_k + R_k,$$

Note that $\Phi_k = -\mathcal{H}_E(\rho_k)^{-1} \mathcal{G}(\rho_k)^{-1} \frac{\delta E}{\delta \rho_k}$. Hence, it follows

$$\mathcal{H}_E(\rho_k) \tau^{-1} T_{k+1} = \mathcal{H}_E(\rho_k) T_k + \mathcal{G}(\rho_k)^{-1} \frac{\delta E}{\delta \rho_k} - \mathcal{H}_E(\rho_k) R_k.$$

For arbitrary $\Psi \in T_{\rho_k}^* \mathcal{P}(\Omega)$, we have

$$\begin{aligned} & \nabla^2 E(\rho_k)(\Psi, \tau^{-1} T_{k+1}) \\ &= \int \Psi \mathcal{H}_E(\rho_k) \tau^{-1} T_{k+1} dx \\ &= \int \Psi (\mathcal{H}_E(\rho_k) T_k + \mathcal{G}(\rho_k)^{-1} \frac{\delta E}{\delta \rho_k} - \mathcal{H}_E(\rho_k) R_k) dx \\ &= \nabla^2 E(\rho_k)(\Psi, T_k) + \nabla E(\rho_k)(\Psi) - \nabla^2 E(\rho_k)(\Psi, R_k) \\ &= -\frac{1}{2} \nabla^3 E(\text{Exp}_{\rho_k}^\lambda)(\tau_\lambda \Psi, \tau_\lambda T_k, \tau_\lambda T_k) - \nabla^2 E(\rho_k)(\Psi, R_k). \end{aligned} \tag{26}$$

Here the last equality comes from Lemma 4. Based on the definition of parallelism, we notice the fact

$$\|\tau_\lambda \Psi\|_{\text{Exp}_{\rho_k}^\lambda(\Phi_k)} = \|\Psi\|_{\rho_k}, \quad \forall \Psi \in T_{\rho_k}^* \mathcal{P}(\Omega).$$

Taking $\Psi = \tau^{-1} T_{k+1}$ in (26), applying Assumption 1 and utilizing Lemma 3 yields

$$\begin{aligned} & \delta_1 \|\tau^{-1} T_{k+1}\|_{\rho_k}^2 \leq |\nabla^2 E(\rho_k)(\tau^{-1} T_{k+1}, \tau^{-1} T_{k+1})| \\ & \leq \frac{1}{2} \left| \nabla^3 E(\text{Exp}_{\rho_k}^\lambda)(\tau_\lambda \tau^{-1} T_{k+1}, \tau_\lambda T_k, \tau_\lambda T_k) \right| + |\nabla^2 E(\rho_k)(\tau^{-1} T_{k+1}, R_k)| \\ & \leq \frac{1}{2} \left| \nabla^3 E(\text{Exp}_{\rho_k}^\lambda)(\tau_\lambda \tau^{-1} T_{k+1}, \tau_\lambda T_k, \tau_\lambda T_k) \right| \\ & \quad + \sqrt{|\nabla^2 E(\rho_k)(R_k, R_k)| |\nabla^2 E(\rho_k)(\tau_\lambda \tau^{-1} T_{k+1}, \tau_\lambda \tau^{-1} T_{k+1})|} \\ & \leq \delta_3 \|\tau_\lambda T_k\|_{\text{Exp}_{\rho_k}^\lambda(\Phi_k)}^2 \|\tau_\lambda \tau^{-1} T_{k+1}\|_{\text{Exp}_{\rho_k}^\lambda(\Phi_k)} + \delta_2 \|\tau^{-1} T_{k+1}\|_{\rho_k} \|R_k\|_{\rho_k} \\ & = \delta_3 \|T_k\|_{\rho_k}^2 \|\tau^{-1} T_{k+1}\|_{\rho_k} + \delta_2 \|\tau^{-1} T_{k+1}\|_{\rho_k} \|R_k\|_{\rho_k}. \end{aligned}$$

Hence, it follows

$$\|T_{k+1}\|_{\rho_{k+1}} = \|\tau^{-1} T_{k+1}\|_{\rho_k} \leq \frac{\delta_3}{\delta_1} \|T_k\|_{\rho_k}^2 + \frac{\delta_2}{\delta_1} \|R_k\|_{\rho_k}.$$

In order to provide an estimation on $\|R_k\|_{\rho_k}$, we introduce Lemma 5.

Lemma 5. *We have following estimations*

$$\|\Phi_k\|_{\rho_k} = O(\|T_k\|_{\rho_k}), \quad \|T_{k+1}\|_{\rho_{k+1}} = O(\|T_k\|_{\rho_k}).$$

Proof. From Assumption 1 and Lemma 3, it follows that

$$\begin{aligned} \|\Psi\|_{\rho_k} \left\| \frac{\delta E}{\delta \rho_k} \right\|_{\rho_k} &\geq \left| \int \Psi \mathcal{G}(\rho_k)^{-1} \frac{\delta E}{\delta \rho_k} dx \right| \\ &= |\nabla^2 E(\rho_k)(\Psi, \Phi_k)| \geq \delta_1 \|\Psi\|_{\rho_k} \|\Phi_k\|_{\rho_k}. \end{aligned}$$

We also notice that from Lemma 4,

$$\begin{aligned} \left\| \frac{\delta E}{\delta \rho_k} \right\|_{\rho_k}^2 &= \nabla E(\rho_k) \left(\frac{\delta E}{\delta \rho_k} \right) \\ &= \nabla^2 E(\rho_k) \left(T_k, \frac{\delta E}{\delta \rho_k} \right) + O \left(\|T_k\|_{\rho_k}^2 \left\| \frac{\delta E}{\delta \rho_k} \right\|_{\rho_k} \right) \\ &= O \left(\|T_k\|_{\rho_k} \left\| \frac{\delta E}{\delta \rho_k} \right\|_{\rho_k} \right). \end{aligned}$$

As a result, we have $\|\Phi_k\|_{\rho_k} = O \left(\left\| \frac{\delta E}{\delta \rho_k} \right\|_{\rho_k} \right) = O(\|T_k\|_{\rho_k})$. We also note the triangle inequality

$$|\|T_k\|_{\rho_k} - \|\Phi_k\|_{\rho_k}| \leq \|T_{k+1}\|_{\rho_{k+1}} \leq \|T_k\|_{\rho_k} + \|\Phi_k\|_{\rho_k}.$$

This yields $\|T_{k+1}\|_{\rho_{k+1}} = O(\|T_k\|_{\rho_k})$. \square

We finally show the estimation of $\|R_k\|_{\rho_k}$.

Lemma 6. *For all $\Psi \in \mathcal{T}_{\rho_k}^* \mathcal{P}(\Omega)$, it follows*

$$\int \Psi \mathcal{G}(\rho_k)^{-1} R_k dx = O(\|\Psi\|_{\rho_k} \|T_k\|_{\rho_k}^2).$$

Proof. Based on the first-order approximation of the exponential map and the parallelsim, we have the following estimations

$$\begin{aligned} \int \Psi(\rho^* - \rho_k) dx &= \int \Psi \mathcal{G}(\rho_k)^{-1} T_k dx + O(\|\Psi\|_{\rho_k} \|T_k\|_{\rho_k}^2). \\ \int \Psi(\rho_{k+1} - \rho_k) dx &= \int \Psi \mathcal{G}(\rho_k)^{-1} \Phi_k dx + O(\|\Psi\|_{\rho_k} \|\Phi_k\|_{\rho_k}^2) \\ &= \int \Psi \mathcal{G}(\rho_k)^{-1} \Phi_k dx + O(\|\Psi\|_{\rho_k} \|T_k\|_{\rho_k}^2). \end{aligned}$$

And

$$\begin{aligned}
& \int \Psi(\rho^* - \rho_{k+1})dx = \int \Psi \mathcal{G}(\rho_{k+1})^{-1} T_{k+1} dx + O(\|\Psi\|_{\rho_{k+1}} \|T_{k+1}\|_{\rho_{k+1}}^2) \\
& = \int \tau^{-1} \Psi \mathcal{G}(\rho_k)^{-1} \tau^{-1} T_{k+1} dx + O(\|\Psi\|_{\rho_k} \|T_{k+1}\|_{\rho_{k+1}}^2 + \|\Psi - \tau^{-1} \Psi\|_{\rho_k} \|T_{k+1}\|_{\rho_{k+1}}^2) \\
& = \int \tau^{-1} \Psi \mathcal{G}(\rho_k)^{-1} \tau^{-1} T_{k+1} dx + O(\|\Psi\|_{\rho_k} \|T_{k+1}\|_{\rho_{k+1}}^2 + \|\Psi\|_{\rho_k} \|\Phi_k\|_{\rho_k} \|T_{k+1}\|_{\rho_{k+1}}^2) \\
& = \int \Psi \mathcal{G}(\rho_k)^{-1} \tau^{-1} T_{k+1} dx + O(\|\Psi\|_{\rho_k} \|T_{k+1}\|_{\rho_{k+1}}^2 + \|\Psi - \tau^{-1} \Psi\|_{\rho_k} \|\tau^{-1} T_{k+1}\|_{\rho_k}) \\
& = \int \Psi \mathcal{G}(\rho_k)^{-1} \tau^{-1} T_{k+1} dx + O(\|\Psi\|_{\rho_k} \|T_{k+1}\|_{\rho_{k+1}}^2 + \|\Psi\|_{\rho_k} \|\Phi_k\|_{\rho_k} \|T_{k+1}\|_{\rho_{k+1}}) \\
& = \int \Psi \mathcal{G}(\rho_k)^{-1} \tau^{-1} T_{k+1} dx + O(\|\Psi\|_{\rho_k} \|T_k\|_{\rho_k}^2).
\end{aligned}$$

Furthermore, we have $R_k = T_k - \tau^{-1} T_{k+1} - \Phi_k$ and

$$\int \Psi(\rho^* - \rho_k) dx - \int \Psi(\rho^* - \rho_{k+1}) dx - \int \Psi(\rho_{k+1} - \rho_k) dx = 0.$$

This completes the proof. \square

Taking $\Psi = R_k$ in Lemma 5 yields $\|R_k\|_{\rho_k} = O(\|T_k\|_{\rho_k}^2)$. We also note that $\|T_k\|_{\rho_k}^2 = \mathcal{D}(\rho_k, \rho^*)^2$. As a result, we have

$$\mathcal{D}(\rho_{k+1}, \rho^*) \leq \frac{\delta_2}{\delta_1} \mathcal{D}(\rho_k, \rho^*)^2 + \frac{\delta_3}{\delta_1} \|R_k\|_{\rho_k} = O(\mathcal{D}(\rho_k, \rho^*)^2).$$

Remark 7. We follow the proof technique in (Smith, 1994, Section 4, Theorem 4.4). Nevertheless, our estimation of $\|R_k\|_{\rho_k}$ is much coarser. With future developments in the theories of curvature estimations and parallelism over density manifold, we expect to prove that $\|R_k\|_{\rho_k} = O(\mathcal{D}(\rho_k, \rho^*)^3)$. The other issue is that our proof is based on the formulation in probability space. In practice, our algorithm is often formulated into samples. In a future work, we shall conduct related proofs in term of samples.

7. PARTICLE IMPLEMENTATION OF WASSERSTEIN NEWTON'S METHOD

In this section, we design sampling efficient implementations of Wasserstein Newton's method. Focusing on Wasserstein Newton's flow of KL divergence, we introduce a variational formulation for computing the Wasserstein Newton's direction. By restricting the Newton's direction in a linear subspace, we derive a sampling efficient algorithm. We also provide a modified algorithm to simplify the calculation of the Newton's direction. Besides, a hybrid method between Newton's Langevin dynamics and overdamped Langevin dynamics is provided.

We briefly review update rules of Newton's methods and hybrid methods in Euclidean space. In each iteration, the update rule of Newton's method follows

$$x_{k+1} = x_k + \alpha_k p_k, \quad p_k = -\nabla^2 f(x_k)^{-1} \nabla f(x).$$

Suppose that $f(x)$ is strictly convex. Namely, $\nabla^2 f(x)$ is positive definite for all $x \in \mathbb{R}^n$. To compute the Newton's direction p_k , it is equivalent to solve the following variational

problem

$$\min_{p \in \mathbb{R}^n} p^T \nabla^2 f(x_k) p + 2 \nabla f(x_k)^T p.$$

In practice, the Newton's direction may not lead to the decrease in the objective function, especially when $f(x)$ is non-convex. Nevertheless, the Newton's method often converges when the update is close to the minimizer. One way to overcome this problem is the hybrid method. Consider a hybrid update of the Newton's direction and the gradient's direction

$$x_{k+1} = x_k + \alpha_k p_k - \alpha_k \lambda_k \nabla f(x_k),$$

where $\lambda_k > 0$ is a parameter.

Following above ideas in Euclidean space, we present a particle implementation of information Newton's method. Here we connect density $\rho_k \in \mathcal{P}(\Omega)$ with a particle system $\{x_k^i\}_{i=1}^N$. Namely, we assume that the distribution $\{x_k^i\}_{i=1}^N$ follows $\rho_k(x)$. Here ρ_k can be approximated by the average of delta measures $\frac{1}{N} \sum_{i=1}^N \delta(x - x_k^i)$. We update each particle by

$$x_{k+1}^i = x_k^i + \alpha_k \nabla \Phi_k(x_k^i), \quad i = 1, 2, \dots, N.$$

Here Φ_k is the solution to Wasserstein Newton's direction equation (3). We next formulate a variational formulation for estimating the Newton's direction as follows.

Proposition 12. *Suppose that $\mathcal{H} : T_\rho^* \mathcal{P}(\Omega) \rightarrow T_\rho \mathcal{P}$ is a linear self-adjoint operator and \mathcal{H} is positive definite. Let $u \in T_\rho \mathcal{P}$. Then the minimizer of variational problem*

$$\min_{\Phi \in T_\rho^* \mathcal{P}(\Omega)} J(\Phi) = \int (\Phi \mathcal{H} \Phi - 2u \Phi) dx,$$

satisfies $\mathcal{H} \Phi = u$, where $\Phi \in T_\rho^* \mathcal{P}(\Omega)$.

Proof. Since \mathcal{H} is linear and self-adjoint, then the optimal solution of satisfies

$$0 = \frac{\delta J}{\delta \Phi} = 2\mathcal{H} \Phi - 2u.$$

Hence, Φ satisfies $\mathcal{H} \Phi = u$. On the other hand, let Φ satisfy $\mathcal{H} \Phi = u$. Then, for any $\Psi \in T_\rho^* \mathcal{P}(\Omega)$, it follows

$$\begin{aligned} J(\Phi + \Psi) &= \int ((\Phi + \Psi) \mathcal{H}(\Phi + \Psi) - 2u(\Phi + \Psi)) dx \\ &= \int (\Phi \mathcal{H} \Phi - 2u \Phi) dx + \int (\Psi \mathcal{H} \Psi - 2u \Psi - 2\Psi \mathcal{H} \Phi) dx \\ &= J(\Phi) + \int \Psi \mathcal{H} \Psi dx \geq J(\Phi). \end{aligned}$$

The last inequality is based on the fact that \mathcal{H} is positive definite. Hence, Φ is the optimal solution to the proposed variational problem. This completes the proof. \square

Suppose that f is strongly convex, or equivalent, $\nabla^2 f(x)$ is positive definite for $x \in \Omega$. Then, the operator $\mathcal{H}_E(\rho)$ defined in (13) is positive definite. Proposition 12 indicates that solving Wasserstein Newton's direction equation (3) is equivalent to optimizing the following variational problem.

$$\min_{\Phi \in T_{\rho_k}^* \mathcal{P}(\Omega)} J(\Phi) = \int \left(\|\nabla^2 \Phi\|_F^2 + \|\nabla \Phi\|_{\nabla^2 f}^2 + 2 \langle \nabla f + \nabla \log \rho_k, \nabla \Phi \rangle \right) \rho_k dx.$$

Here we denote $\|v\|_A^2 = v^T A v$. For general f , suppose that there exists $\epsilon \geq 0$ such that $\nabla^2 f(x) + \epsilon I$ is strictly convex for $x \in \Omega$. Then, we consider a regularized problem

$$\min_{\Phi \in T_{\rho_k}^* \mathcal{P}(\Omega)} J(\Phi) = \int \left(\|\nabla^2 \Phi\|_F^2 + \|\nabla \Phi\|_{\nabla^2 f + \epsilon I}^2 + 2 \langle \nabla f + \nabla \log \rho_k, \nabla \Phi \rangle \right) \rho_k dx. \quad (27)$$

Remark 8. *The regularized problem (27) is equivalent to*

$$\min_{\Phi \in T_{\rho_k}^* \mathcal{P}(\Omega)} J(\Phi) + \epsilon \int \|\nabla \Phi\|^2 \rho_k dx = J(\Phi) + \epsilon \|\Phi\|_{\rho_k}^2.$$

Namely, we penalize the squared norm of Φ , which is induced by the Wasserstein metric.

Based on (27), we are able to present a particle implementation of the Newton's direction. For the case where ρ_k is Gaussian and ρ^* is Gaussian, we have

$$\xi_k(x) = -\bar{\Sigma}_k^{-1}(x - \bar{x}_k), \quad (28)$$

where \bar{x}_k and $\bar{\Sigma}_k$ are mean and empirical covariance matrix of $\{x_k^i\}_{i=1}^N$, respectively. For general ρ_k and ρ^* , we can approximate $\nabla \log \rho_k$ via kernel density estimation (KDE) (Gretton et al., 2012). Namely, we approximate $\nabla \log \rho_k$ by

$$\xi_k(x) = \frac{\sum_{i=1}^N \nabla_y k(x, x_k^i)}{\sum_{i=1}^N \nabla k(x, x_k^i)}.$$

Here $k(x, y)$ is a given positive kernel. A typical choice of $k(x, y)$ is a Gaussian kernel with bandwidth $h > 0$, such that

$$k(x, y) = (2\pi h)^{-n/2} \exp\left(-\frac{\|x - y\|^2}{2h}\right).$$

The bandwidth h is critical to the estimation of $\nabla \log \rho_k$.

Remark 9. *We can also approximate $\nabla \log \rho_k$ via a kernel function by the blob method (Carrillo et al., 2019) and the diffusion map (Taghvaei and Mehta, 2019).*

7.1. Affine Wasserstein Newton's method. In high dimensional sample space, directly solving (27) for $\Phi \in T_{\rho_k}^* \mathcal{P}(\Omega)$ can be difficult. In this subsection, we present a practical method to approximate the Newton's direction Φ_t^{Newton} . To deal with this, we restrict Φ in infinite dimensional function space $\mathcal{F}(\Omega)$ to a finite-dimensional subspace. Here the subspace is designed as the following linear vector space spanned by basis functions.

Consider $\Psi = \text{span}\{\psi_i\}_{i=1}^m$, where $\psi_i : \Omega \rightarrow R$ are given basis functions. Namely, we assume that $\Phi(x)$ is a linear combination of ψ_1, \dots, ψ_m , such that

$$\Phi(x) = \langle \mathbf{a}, \psi(x) \rangle = \sum_{i=1}^m a_i \psi_i(x),$$

where $\mathbf{a} \in \mathbb{R}^m$ and $\psi(x) = [\psi_1(x), \psi_2(x), \dots, \psi_m(x)]$.

Proposition 13. *Suppose that $\Phi(x) = \langle \mathbf{a}, \psi(x) \rangle$. Then, the optimization problem (27) constrained in $\Phi \in \Psi$ turns to be*

$$\min_{\mathbf{a} \in \mathbb{R}^m} J(\mathbf{a}) = \mathbf{a}^T (\mathbf{B}_k + \mathbf{D}_k) \mathbf{a} + 2\mathbf{c}_k^T \mathbf{a},$$

where $\mathbf{B}_k, \mathbf{D}_k \in \mathbb{R}^{m \times m}$ and $\mathbf{c}_k \in \mathbb{R}^m$. The detailed formulations of $\mathbf{B}_k, \mathbf{D}_k$ and \mathbf{c}_k are provided as follows.

$$\begin{aligned}\mathbf{B}_k &= \frac{1}{N} \sum_{i=1}^N \nabla \psi(x_k^i) (\nabla^2 f(x_k^i) + \epsilon I) (\nabla \psi(x_k^i))^T, \\ \mathbf{D}(x)_{j_1, j_2} &= \frac{1}{N} \sum_{i=1}^N \text{tr}(\nabla^2 \psi_{j_1}(x_k^i) \nabla^2 \psi_{j_2}(x_k^i)), \\ \mathbf{c}(x) &= \frac{1}{N} \sum_{i=1}^N \nabla \psi(x_k^i) (\nabla f(x_k^i) + \xi_k(x_k^i)).\end{aligned}$$

If $\mathbf{B}_k + \mathbf{D}_k$ is positive definite, the optimal solution follows $\mathbf{a} = -(\mathbf{B}_k + \mathbf{D}_k)^{-1} \mathbf{c}_k$. The optimal solution Φ^{Newton} follows $\Phi^{\text{Newton}}(x) = \langle \mathbf{a}, \psi(x) \rangle$.

Proof. We denote the Jacobian $\nabla \psi(x) \in \mathbb{R}^{n \times m}$. As a result, $J(\mathbf{a})$ turns to be

$$J(\mathbf{a}) = \left\{ \frac{1}{N} \sum_{i=1}^N \left\| \sum_{j=1}^m a_j \nabla^2 \psi_j(x_k^i) \right\|_F^2 + \mathbf{a}^T \mathbf{B}(x_k^i) \mathbf{a} + 2 \mathbf{a}^T \mathbf{c}(x_k^i), \mathbf{a} \right\}.$$

We can further compute that

$$\left\| \sum_{j=1}^m \mathbf{a}_j \nabla^2 \psi_j(x_k^i) \right\|_F^2 = \sum_{j_1=1}^m \sum_{j_2=1}^m \mathbf{a}_{j_1} \nabla^2 \psi_{j_1}(x_k^i) \nabla^2 \psi_{j_2}(x_k^i) \mathbf{a}_{j_2} = \mathbf{a}^T \mathbf{D}(x_k^i) \mathbf{a}.$$

This completes the proof. \square

This affine approximation technique has been used in approximating natural gradient direction in (Li et al., 2019). Hence, we call our method affine information Newton's method.

We further consider a special case where ψ_i are linear and quadratic polynomials. Namely, we set $m = n(n+3)/2$ and

$$\psi_i(x) = x_i, \quad 1 \leq i \leq n, \quad \psi_{n+i(i-1)/2+j} = x_i x_j, \quad 1 \leq j \leq i \leq n.$$

In other words, we assume that $\Phi(x)$ takes the form $\Phi(x) = \frac{1}{2} x S x + b^T x$, where $S \in \mathbb{R}^{n \times n}$ is a symmetric matrix. For simplicity, we denote $v_k^i = \nabla f(x_k^i) + \xi_k(x_k^i)$. Then, the variational problem (27) turns to be

$$\min_{S \in \mathbb{S}^n, b \in \mathbb{R}^n} J(S, b) = \text{tr}(S^2) + \frac{1}{N} \sum_{i=1}^N \left(\|S x_k^i + b\|_{\nabla^2 f(x_k^i) + \epsilon I}^2 + 2 \langle S x_k^i + b, v_k^i \rangle \right). \quad (29)$$

We further restrict S to be a diagonal matrix $S = \text{diag}(s)$, where $s \in \mathbb{R}^n$. Here we use $\text{diag}(s)$ to represent the diagonal matrix in $\mathbb{R}^{n \times n}$ with elements in s as its diagonal

components. Then, we can write the objective function to be

$$\begin{aligned}
& J(s, b) \\
&= \|s\|^2 + \frac{1}{N} \sum_{i=1}^N \text{tr}((\text{diag}(x_k^i)s + b)^T (\nabla^2 f(x_k^i) + \epsilon I)(\text{diag}(x_k^i)s + b)) + 2 \langle \text{diag}(x_k^i)s + b, v_k^i \rangle \\
&= \begin{bmatrix} s \\ b \end{bmatrix}^T \mathbf{H}_k \begin{bmatrix} s \\ b \end{bmatrix} + 2 \begin{bmatrix} s \\ b \end{bmatrix}^T u_k.
\end{aligned}$$

where we denote $\mathbf{H}_k \in \mathbb{R}^{2n \times 2n}$ via

$$\mathbf{H}_k = \begin{bmatrix} I + \frac{1}{N} \sum_{i=1}^N \text{diag}(x_k^i) \nabla^2 f(x_k^i) \text{diag}(x_k^i) & \frac{1}{N} \sum_{i=1}^N \text{diag}(x_k^i) \nabla^2 f(x_k^i) \\ \frac{1}{N} \sum_{i=1}^N \nabla^2 f(x_k^i) \text{diag}(x_k^i) & \frac{1}{N} \sum_{i=1}^N \nabla^2 f(x_k^i) \end{bmatrix},$$

and $u_k \in \mathbb{R}^{2n}$ via

$$u_k = \begin{bmatrix} \frac{1}{N} \sum_{i=1}^N \text{diag}(x_k^i) v_k^i \\ \frac{1}{N} \sum_{i=1}^N v_k^i \end{bmatrix}.$$

Hence, the optimal solution for minimizing $J(s, b)$ follows

$$\begin{bmatrix} s_k \\ b_k \end{bmatrix} = -(\mathbf{H}_k)^{-1} u_k.$$

The overall algorithm is summarized in 1.

Algorithm 1 Particle implementation of affine Wasserstein Newton's method

Require: initial positions $\{x_0^i\}_{i=1}^N$, $\epsilon \geq 0$, step sizes α_k , maximum iteration K .

- 1: Set $k = 0$.
- 2: **while** $k < K$ and the convergence criterion is not met **do**
- 3: Compute $v_k^i = \nabla f(x_k^i) + \xi_k(x_k^i)$. Here ξ_k is an approximation of $\nabla \log \rho_k$.
- 4: Calculate \mathbf{H}_k by

$$\mathbf{H}_k = \begin{bmatrix} I + \frac{1}{N} \sum_{i=1}^N \text{diag}(x_k^i) \nabla^2 f(x_k^i) \text{diag}(x_k^i) & \frac{1}{N} \sum_{i=1}^N \text{diag}(x_k^i) \nabla^2 f(x_k^i) \\ \frac{1}{N} \sum_{i=1}^N \nabla^2 f(x_k^i) \text{diag}(x_k^i) & \frac{1}{N} \sum_{i=1}^N \nabla^2 f(x_k^i) \end{bmatrix},$$

and formulate u_k by

$$u_k = \begin{bmatrix} \frac{1}{N} \sum_{i=1}^N \text{diag}(x_k^i) v_k^i \\ \frac{1}{N} \sum_{i=1}^N v_k^i \end{bmatrix}.$$

- 5: Compute s_k and b_k by

$$\begin{bmatrix} s_k \\ b_k \end{bmatrix} = -(\mathbf{H}_k)^{-1} u_k.$$

- 6: Update particle positions by

$$x_{k+1}^i = x_k^i + \alpha_k (\text{diag}(s_k) x_k^i + b_k).$$

- 7: Set $k = k + 1$.
 - 8: **end while**
-

7.2. Modified affine Wasserstein Newton's method. Optimizing $J(S, b)$ defined in (29) for $S \in \mathbb{S}^n$ can be challenging and time-consuming. Here we consider a modification of Newton's method. In other words, we consider the following problem.

$$\min_{S \in \mathbb{S}^n, b \in \mathbb{R}^n} \hat{J}(S, b) = \text{tr}(S^2) + \frac{1}{N} \sum_{i=1}^N (\|Sx_k^i + b\|_{F_k}^2 + 2 \langle Sx_k^i + b, v_k^i \rangle). \quad (30)$$

Here $F_k = \frac{1}{N} \sum_{i=1}^N \nabla^2 f(x_k^i) + \epsilon I$, where $\epsilon \geq 0$ is a parameter. Namely, we use the averaged Hessian F_k to replace the Hessian $\nabla^2 f(x_k^i) + \epsilon I$ of individual particle. We notice that this modification does not change the original variational problem (29) if ρ^* is a Gaussian distribution.

With this modification, we can compute the direction by solving a quadratic matrix optimization problem as follows.

Proposition 14. *The optimal solution to (30) follows*

$$b_k = -\frac{1}{N} \sum_{i=1}^N (S_k x_k^i + F_k^{-1} v_k^i),$$

and S_k is the solution to the quadratic matrix optimization problem

$$\min_{S \in \mathbb{S}^n} 2 \text{tr}(S^2) + \text{tr}(S \bar{\Sigma}_k S F_k) + \text{tr}(S \bar{F}_k S \bar{\Sigma}_k) - 2 \text{tr}(\bar{T}_k S). \quad (31)$$

Here $\bar{\Sigma}_k$ is an empirical covariance matrix of x_k^i and \bar{T}_k is an empirical covariance matrix between x_k^i and v_k^i .

Proof. For a fixed S , the optimal b for minimizing $\hat{J}(S, b)$ defined in (30) follows

$$b = -\frac{1}{N} \sum_{i=1}^N (Sx_k^i + F_k^{-1} v_k^i).$$

For simplicity, let $\bar{x}_k = \frac{1}{N} \sum_{i=1}^N x_k^i$ and $\bar{v}_k = \frac{1}{N} \sum_{i=1}^N v_k^i$. Substituting b^* into the optimization problem (30) renders

$$\min_{S \in \mathbb{S}^n} \text{tr}(S^2) + \frac{1}{N} \sum_{i=1}^N (\|Sx_k^i - S\bar{x}_k - F_k^{-1} \bar{v}_k\|_{F_k}^2 + 2 \langle Sx_k^i - S\bar{x}_k - F_k^{-1} \bar{v}_k, v_k^i \rangle).$$

Let $\tilde{x}_k^i = x_k^i - \bar{x}_k$ and $\tilde{v}_k^i = v_k^i - \bar{v}_k$. Then, the above problem is equivalent to

$$\min_{S \in \mathbb{S}^n} \text{tr}(S^2) + \frac{1}{N} \sum_{i=1}^N (\|S\tilde{x}_k^i\|_{F_k}^2 + 2 \langle S\tilde{x}_k^i, \tilde{v}_k^i \rangle).$$

Moreover, let $\bar{\Sigma}_k = \frac{1}{N} \sum_{i=1}^N \tilde{x}_k^i (\tilde{x}_k^i)^T$ and $\bar{T}_k = \frac{1}{2N} \sum_{i=1}^N (\tilde{v}_k^i (\tilde{x}_k^i)^T + \tilde{x}_k^i (\tilde{v}_k^i)^T)$. Then, problem (30) is equivalent to problem (31). \square

Because (31) is a quadratic optimization problem on \mathbb{S}^n , it can be efficiently solved by the conjugate gradient (CG) method. Detailed description of the CG method can be found in Appendix B. Denote the solution by S_k . The update rule for x_{k+1}^i follows

$$x_{k+1}^i = x_k^i + \alpha_k (S_k x_k^i + b_k) = x_k^i + \alpha_k (S_k \tilde{x}_k^i - F_k^{-1} \bar{v}_k).$$

The overall algorithm is summarized in Algorithm 2

Algorithm 2 Particle implementation of modified affine Wasserstein Newton's method

Require: initial positions $\{x_1^i\}_{i=1}^N$, $\epsilon \geq 0$, step sizes α_k , maximum iteration K .

- 1: Set $k = 1$ and $S_0 = I$.
- 2: **while** $k \leq K$ and the convergence criterion is not met **do**
- 3: Calculate $v_k^i = \nabla f(x_k^i) + \xi_k(x_k^i)$. Here ξ_k is an approximation of $\nabla \log \rho_k$.
- 4: Compute the averaged Hessian with regularization by $F_k = \epsilon I + \frac{1}{N} \sum_{i=1}^N \nabla^2 f(x_k^i)$.
- 5: Compute the means $\bar{x}_k = \frac{1}{N} \sum_{i=1}^N x_k^i$ and $\bar{v}_k = \frac{1}{N} \sum_{i=1}^N v_k^i$.
- 6: Let $\tilde{x}_k^i = x_k^i - \bar{x}_k$ and $\tilde{v}_k^i = v_k^i - \bar{v}_k$.
- 7: Compute $\bar{\Sigma}_k = \frac{1}{N} \sum_{i=1}^N \tilde{x}_k^i (\tilde{x}_k^i)^T$ and $\bar{T}_k = \frac{1}{2N} \sum_{i=1}^N (\tilde{v}_k^i (\tilde{x}_k^i)^T + \tilde{x}_k^i (\tilde{v}_k^i)^T)$.
- 8: Solve S_k from the problem (30) via the CG method using the initial guess S_{k-1} .
- 9: Update particle positions by

$$x_{k+1}^i = x_k^i + \alpha_k (S_k \tilde{x}_k^i - F_k^{-1} \bar{v}_k).$$

10: **end while**

7.3. The hybrid method. In practice, the Newton's direction may not be a descent direction if the update is far away from the minimizer. To overcome this issue, we propose a hybrid update of Newton's direction and gradient direction.

Let $\lambda_k \geq 0$ be a parameter. Here we recall that there are two choices for using the gradient direction. Namely, if we use overdamped Langevin dynamics as gradient direction, the hybrid update rule follows

$$x_{k+1}^i = x_k^i + \alpha_k (S_k x_k^i + b_k) + \sqrt{2\lambda_k \alpha_k} B_k, \quad (32)$$

where $B_k \sim \mathcal{N}(0, I)$. If we use Lagrangian Langevin dynamics as gradient direction, the hybrid update rule satisfies

$$x_{k+1}^i = x_k^i + \alpha_k (S_k x_k^i + b_k - \lambda_k v_k^i). \quad (33)$$

Remark 10. *It worths mentioning that our algorithm corresponds to the following hybrid Langvien dynamics*

$$dX_t = (\nabla \Phi_t^{\epsilon-\text{Newton}} - \lambda_t \nabla f) dt + \sqrt{2\lambda_t} dB_t,$$

where B_t is the standrad Brownian motion, $\lambda_t, \epsilon > 0$ are given parameters and $\Phi_t^{\epsilon-\text{Newton}}$ is the minimizer of variational problem (27).

8. NUMERICAL EXPERIMENTS

In this section, we present numerical experiments to demonstrate the strength of information Newton's flows.

8.1. Toy examples. We compare particle implementations among affine Wasserstein Newton's method (WNewton), modified affined Wasserstein Newton's method (mWNewton), Wasserstein gradient flow (WGF) and the Hessian Approximated Lagrangian Langevin dynamics (HALLD). We notice that the update rule of WGF satisfies

$$x_{k+1}^i = x_k^i + \alpha_k (-\nabla f(x_k^i) - \xi_k(x_k^i)).$$

The update rule of HALLD follows

$$x_{k+1}^i = x_k^i + \alpha_k \nabla^2 f(x_k^i)^{-1} (-\nabla f(x_k^i) - \xi_k(x_k^i)).$$

We note that the density evolutions of HALLD and HAMCMC are identical to each other. In other words, we replace the Brownian motion in HAMCMC by ξ_k in HALLD. Here ξ_k is an approximation of $\nabla \log \rho_k$. For all compared methods, we use constant step sizes. For the calculation of ξ_k , we apply KDE with Gaussian kernels and the kernel bandwidth is selected by Brownian Motion method (Wang and Li, 2019)[section 5.1]. This method adaptively learns the bandwidth from samples generated by Brownian motions.

We first consider a 1D target density $\rho^*(x) \propto \exp(-f(x))$, where $f(x) = \frac{1}{2}(x^2 - 1)^2$. For WGF, we set $\alpha_k = 0.01$. For WNewton and mWNewton, we let $\alpha_k = 1$, $\epsilon = 0$ and $\lambda_k = 0$. Namely, we do not apply the hybrid update. For HALLD, we set $\alpha = 0.01$. The sample number follows $N = 100$. The initial distribution follows $\mathcal{N}(0, 0.01)$. We plot the distribution after 2, 5, 10, 20 iterations in Figure 2. Although we use affine approximations to compute the Newton’s direction, WNewton tends to converge to the target density and it is faster than WGF. Even with a small step size, some samples generated by HALLD tends to go to infinity. This is because $f(x)$ is not a convex function.

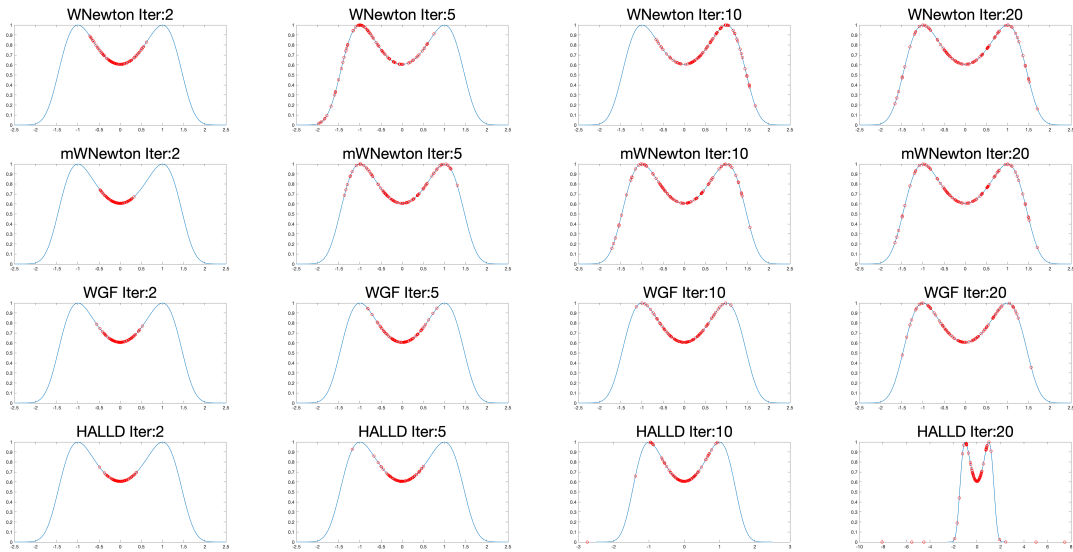


FIGURE 2. Comparison among WNewton, mWNewton, WGF and HALLD in 1D toy example. Left to right: sample distribution after 2, 5, 10, 20 iterations.

Then, we let the target density ρ^* to be a toy bimodal distribution (Rezende and Mohamed, 2015) in \mathbb{R}^2 . For WGF, we set $\alpha_k = 0.1$. For WNewton and mWNewton, we apply the hybrid update and set $\alpha_k = 0.2$, $\epsilon = 0$ and $\lambda_k = 0.5$. The sample number follows $N = 200$. The initial distribution follows $\mathcal{N}([0, 10]', I)$. We plot the distribution after 5, 10, 20, 40 iterations in Figure 3. HALLD fails because $\nabla^2 f$ becomes singular on certain sample points. We observe that the Wasserstein Newton’s direction helps samples converge faster towards the target density.

8.2. Gaussian families. The target density ρ^* is a Gaussian distribution with zero mean on \mathbb{R}^{100} . The covariance matrix of ρ^* is Σ^* and $W^* = (\Sigma^*)^{-1}$. Let L and β be the largest/smallest eigenvalue of W^* . The condition number of W^* is defined as $\kappa = L/\beta$.

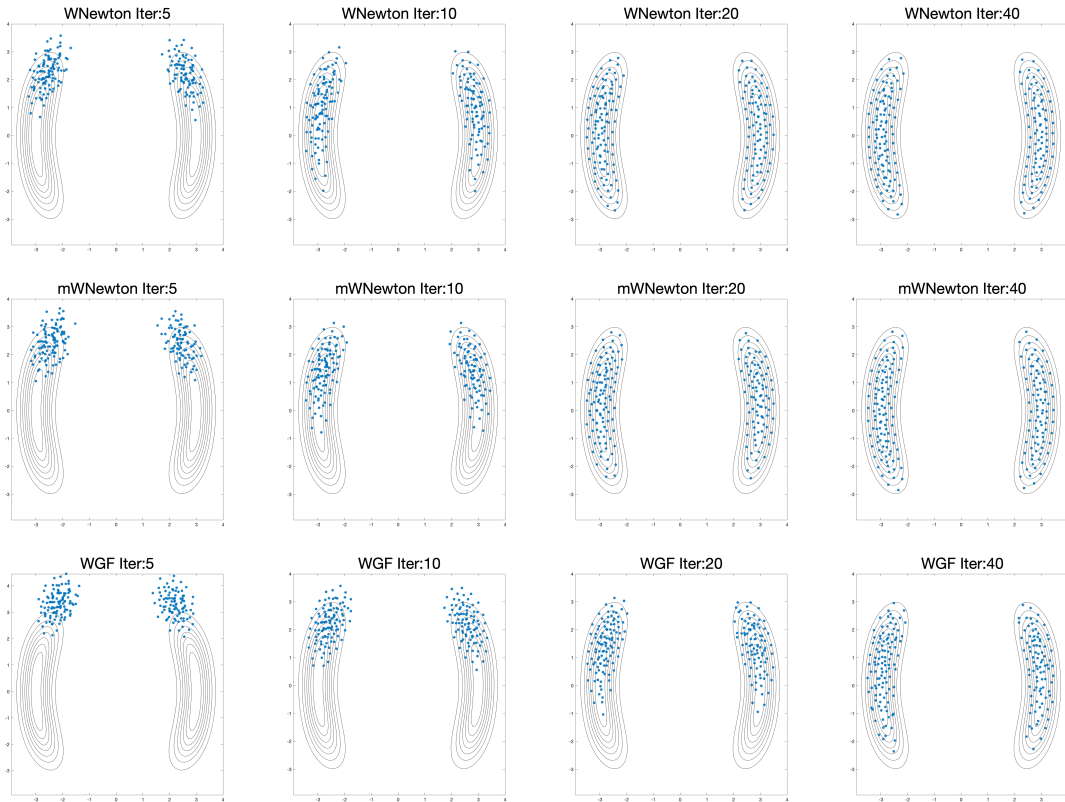


FIGURE 3. Comparison among WNewton, mWNewton and WGF in 2D toy example. Left to right: sample distribution after 5, 10, 20, 40 iterations.

The initial distribution follows $\mathcal{N}(0, I)$ and the number of particle $N = 600$. For a Gaussian target density, mWNewton is exactly the Wasserstein Newton’s method. We compare mWNewton with WGF, the particle implementation of Accelerated Information Gradient flow (Wang and Li, 2019, AIG) and HALLD. For WGF and AIG, we set the step size to be $\alpha_k = 1/(2L)$. For AIG, we use the restart technique. For mWNewton, we set $\alpha_k = 1$, $\epsilon = 0$ and $\lambda_k = 0$. Namely, we add no regularization and do not apply the hybrid update. For HALLD, we choose two step sizes $\alpha_k = 1$ and $\alpha_k = 0.5$. For a particle system $\{X_k^i\}_{i=1}^N$, we record the KL divergence $E(\hat{\Sigma}_k)$ (21) using the empirical covariance matrix $\hat{\Sigma}_k$. The results are collected in Figure 4. We observe that mWNewton converges to the optimal distribution in less than 30 iterates, while AIG takes nearly 2000 iterations. In CPU-time, mWNewton also has competitive performance with AIG. With $\alpha_k = 1$, HALLD does not converge while with $\alpha_k = 0.5$, HALLD converges rapidly.

8.3. Bayesian logistic regression. We perform the standard Bayesian logistic regression experiment on the Covertypes dataset, following the settings in (Liu and Wang, 2016). We compare WNewton and mWNewton with MCMC, SVGD (Liu and Wang, 2016), Wnes (Liu et al., 2019), WGF and AIG. For the calculation of ξ_k in WGF, AIG, Wnes, WNewton and mWNewton we use KDE with Gaussian kernel and the bandwidth is selected by the median method, which is the same as (Liu and Wang, 2016). The sample number follows

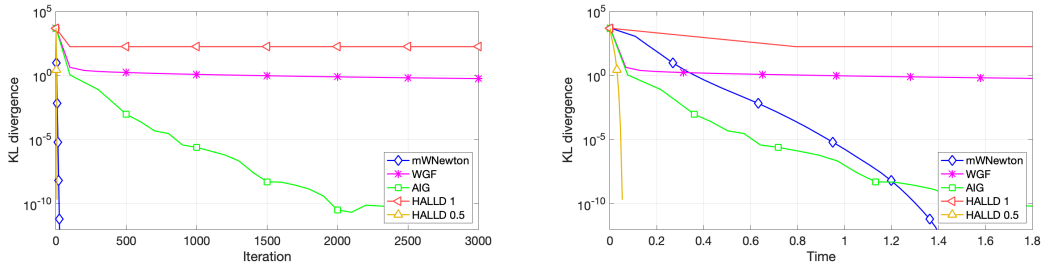


FIGURE 4. Comparison among WNewton, WGF, AIG and HALLD in Gaussian families. The conditional number $\kappa = 2 \times 10^4$. For Newton and HALLD 0.5, the markers are marked for every 5 iterations.

$N = 100$. The mini-batch size for stochastic gradient and Hessian evaluations in each iteration is 100.

We first elaborate on the choice of step sizes. The initial step sizes for the compared methods are given in Table 2. The step size of SVGD is adjusted by Adagrad [cite], which is same as (Liu and Wang, 2016). For WRes, the step size is give by $\tau_l = \tau_0/l^{0.9}$ for $l \geq 1$. For MCMC, WGF and AIG, the step size is multiplied by 0.9 every 100 iterations. For WNewton and mWNewton, the step size is multiplied by 0.82 every 100 iterations.

Method	MCMC	SVGD	Wnes	WGF	AIG	WNewton	mWNewton
Step size α_0	1e-5	0.05	1e-5	1e-5	1e-6	2e-3	2e-3

TABLE 2. Initial step sizes for algorithms in comparison.

We then elaborate on the implementation details of compared methods. The parameters for Wnes are identical to (Liu et al., 2019). For AIG, we apply the adaptive restart technique. For WNewton and mWNewton, we apply the hybrid update and set $\epsilon = 0$, $\lambda_k = 0.005$.

From Figure 5, we observe that AIG and mWNewton has competitive performance in test accuracy and they outperform other methods. Although the performance of WNewton is not stable in first 500 iterations, WNewton achieves larger test log-likelihood value than other methods (Larger is better). And mWNewton has slightly smaller test log-likelihood value than WNewton.

9. CONCLUSION AND DISCUSSION

In this paper, we introduce information Newton’s flows (second-order optimization methods) for optimization problems in probability space arising from Bayesian statistics, inverse problems, and machine learning. Here two information metrics, such as Fisher-Rao metric and Wasserstein-2 metric, are considered. Several examples and convergence analysis of the proposed second-order methods are provided. Following the fact that the Wasserstein gradient flow of KL divergence formulates the Langevin dynamics, we derive the Wasserstein Newton’s flow of KL divergence as Newton’s Langevin dynamics. Focusing on Newton’s Langevin dynamics, we study analytical examples in one-dimensional sample space and Gaussian families. We further propose practical sampling efficient algorithms to

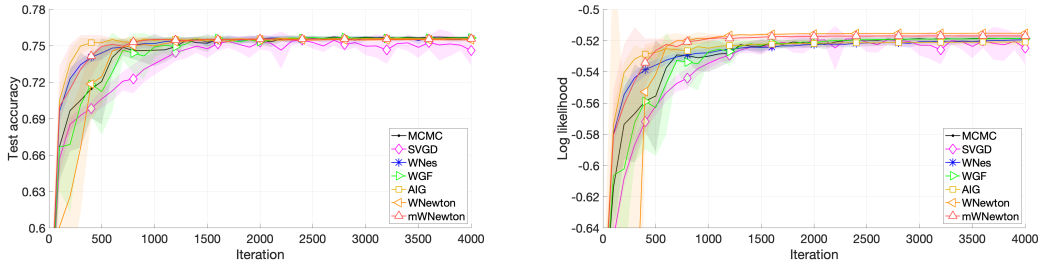


FIGURE 5. Comparison of different methods on Bayesian logistic regression, averaged over 10 independent trials. The shaded areas show the variance over 10 trials. Left: Test accuracy; Right: Test log-likelihood.

implement Newton’s Langevin dynamics. The numerical examples in Bayesian statistics demonstrate the effectiveness of the proposed method.

Our work opens a door to design high-order optimization methods for Bayesian sampling, machine learning and inverse problems. We observe that high-order derivatives from information metrics are very useful in designing sampling efficient optimization methods. In future works, we shall study the following questions. For example, what is the sampling efficient Quasi-Newton’s method for information metrics? Several natural choices of quasi-Newton’s method include the Rank one formulation (SR1) and BFGS. What is the other efficient method to approximate the Wasserstein Newton’s direction? In our paper, we apply the affine method to restrict the Newton’s direction in a finite dimension subspace. We expect to apply kernelized methods to improve the approximation. Lastly, we shall further propose the information Newton’s flow not only for probability space but also for probability models, especially generative models.

REFERENCES

- Amari, S.-I. (1998). Natural gradient works efficiently in learning. *Neural computation*, 10(2):251–276.
- Amari, S.-i. (2016). *Information geometry and its applications*, volume 194. Springer.
- Bakry, D. and Émery, M. (1985). Diffusions hypercontractives. In *Séminaire de Probabilités XIX 1983/84*, pages 177–206. Springer.
- Bernton, E. (2018). Langevin monte carlo and JKO splitting. *arXiv preprint arXiv:1802.08671*.
- Boothby, W. M. (1986). *An introduction to differentiable manifolds and Riemannian geometry*, volume 120. Academic press.
- Carrillo, J. A., Craig, K., and Patacchini, F. S. (2019). A blob method for diffusion. *Calculus of Variations and Partial Differential Equations*, 58(2):53.
- Carrillo, J. A., Lisini, S., Savare, G., and Slepcev, D. (2010). Nonlinear mobility continuity equations and generalized displacement convexity. *J. Funct. Anal.*, 258(4):1273–1309.
- Chen, P., Wu, K., Chen, J., O’Leary-Roseberry, T., and Ghattas, O. (2019). Projected stein variational newton: A fast and scalable bayesian inference method in high dimensions. *arXiv preprint arXiv:1901.08659*.
- Detommaso, G., Cui, T., Marzouk, Y., Spantini, A., and Scheichl, R. (2018). A stein variational newton method. In *Advances in Neural Information Processing Systems*, pages 9169–9179.

- Dolbeault, J., Nazaret, B., and Savaré, G. (2009). A new class of transport distances between measures. *Calculus of Variations and Partial Differential Equations*, 34(2):193–231.
- Garbuno-Inigo, A., Hoffmann, F., Li, W., and Stuart, A. M. (2019). Interacting langevin diffusions: Gradient structure and ensemble kalman sampler. *arXiv preprint arXiv:1903.08866*.
- Gretton, A., Borgwardt, K. M., Rasch, M. J., Schölkopf, B., and Smola, A. (2012). A kernel two-sample test. *Journal of Machine Learning Research*, 13(Mar):723–773.
- Huang, W. (2013). Optimization algorithms on riemannian manifolds with applications.
- Jordan, R., Kinderlehrer, D., and Otto, F. (1998). The variational formulation of the fokker–planck equation. *SIAM journal on mathematical analysis*, 29(1):1–17.
- Kingma, D. P. and Ba, J. (2014). Adam: A method for stochastic optimization. *arXiv preprint arXiv:1412.6980*.
- Lafferty, J. D. (1988). The density manifold and configuration space quantization. *Transactions of the American Mathematical Society*, 305(2):699–741.
- Li, W. (2018). Geometry of probability simplex via optimal transport. *arXiv preprint arXiv:1803.06360*.
- Li, W. (2019). Diffusion hypercontractivity via generalized density manifold. *CoRR*, abs/1907.12546.
- Li, W., Lin, A. T., and Montúfar, G. (2019). Affine natural proximal learning. *Geometric science of information*, 2019.
- Li, W. and Ying, L. (2019). Hessian transport gradient flows. *Research in the Mathematical Sciences*, 6(4):34.
- Liu, C., Zhuo, J., Cheng, P., Zhang, R., and Zhu, J. (2019). Understanding and accelerating particle-based variational inference. In *International Conference on Machine Learning*, pages 4082–4092.
- Liu, C., Zhuo, J., Cheng, P., Zhang, R., Zhu, J., and Carin, L. (2018). Accelerated first-order methods on the wasserstein space for bayesian inference. *arXiv preprint arXiv:1807.01750*.
- Liu, Q. (2017). Stein variational gradient descent as gradient flow. In Guyon, I., Luxburg, U. V., Bengio, S., Wallach, H., Fergus, R., Vishwanathan, S., and Garnett, R., editors, *Advances in Neural Information Processing Systems 30*, pages 3115–3123. Curran Associates, Inc.
- Liu, Q. and Wang, D. (2016). Stein variational gradient descent: A general purpose bayesian inference algorithm. In *Advances in neural information processing systems*, pages 2378–2386.
- Lu, Y., Lu, J., and Nolen, J. (2019). Accelerating langevin sampling with birth-death. *arXiv preprint arXiv:1905.09863*.
- Ma, Y.-A., Chatterji, N., Cheng, X., Flammarion, N., Bartlett, P., and Jordan, M. I. (2019). Is there an analog of nesterov acceleration for mcmc? *arXiv preprint arXiv:1902.00996*.
- Malagò, L., Montrucchio, L., and Pistone, G. (2018). Wasserstein riemannian geometry of positive definite matrices. *arXiv preprint arXiv:1801.09269*.
- Malagò, L. and Pistone, G. (2014). Combinatorial optimization with information geometry: The newton method. *Entropy*, 16(8):4260–4289.
- Martens, J. and Grosse, R. (2015). Optimizing neural networks with kronecker-factored approximate curvature. In *International conference on machine learning*, pages 2408–2417.

- Modin, K. (2016). Geometry of matrix decompositions seen through optimal transport and information geometry. *arXiv preprint arXiv:1601.01875*.
- Ollivier, Y., Arnold, L., Auger, A., and Hansen, N. (2017). Information-geometric optimization algorithms: A unifying picture via invariance principles. *The Journal of Machine Learning Research*, 18(1):564–628.
- Otto, F. (2001). The geometry of dissipative evolution equations: the porous medium equation. *Communications in Partial Differential Equations*, 26(1-2):101–174.
- Otto, F. and Villani, C. (2000). Generalization of an inequality by talagrand and links with the logarithmic sobolev inequality. *Journal of Functional Analysis*, 173(2):361–400.
- Rezende, D. J. and Mohamed, S. (2015). Variational inference with normalizing flows. *arXiv preprint arXiv:1505.05770*.
- Simsekli, U., Badeau, R., Cemgil, T., and Richard, G. (2016). Stochastic quasi-newton langevin monte carlo. In *International Conference on Machine Learning (ICML)*.
- Smith, S. T. (1994). Optimization techniques on riemannian manifolds. *Fields institute communications*, 3(3):113–135.
- Stuart, A. M. (2010). Inverse problems: a bayesian perspective. *Acta numerica*, 19:451–559.
- Taghvaei, A. and Mehta, P. G. (2019). Accelerated flow for probability distributions. *arXiv preprint arXiv:1901.03317*.
- Takatsu, A. (2008). On wasserstein geometry of the space of gaussian measures. *arXiv preprint arXiv:0801.2250*.
- Villani, C. (2003). *Topics in optimal transportation*. American Mathematical Soc.
- Villani, C. (2008). *Optimal transport: old and new*, volume 338. Springer Science & Business Media.
- Wang, Y. and Li, W. (2019). Accelerated information gradient flow. *arXiv preprint arXiv:1909.02102*.
- Wibisono, A. (2019). Proximal langevin algorithm: Rapid convergence under isoperimetry. *arXiv preprint arXiv:1911.01469*.
- Yang, Y. (2007). Globally convergent optimization algorithms on riemannian manifolds: Uniform framework for unconstrained and constrained optimization. *Journal of Optimization Theory and Applications*, 132(2):245–265.

APPENDIX A. SUMMARY OF NEWTON’S FLOWS

In this section, we summarize formulations of Hessian-related operators $\mathcal{H}_E(\rho)$ under both Fisher-Rao metric and Wasserstein metric.

APPENDIX B. CONJUGATE GRADIENT METHOD IN THE SPACE OF SYMMETRIC MATRICES

Let $\mathcal{H} : \mathbb{S}^n \rightarrow \mathbb{S}^n$ to be a positive definite linear operator in the space of symmetric matrices \mathbb{S}^n . For $T \in \mathbb{S}^n$, let us consider the quadratic optimization problem

$$\min_S \text{tr}(S\mathcal{H}S) - 2 \text{tr}(ST).$$

This problem can be easily solved by the conjugate gradient (CG) method, which is given in Algorithm 3. In the particle implementation of the affine information Newton’s method,

Objective functional $E(\rho)$	$\mathcal{H}_E^F(\rho)\Phi$
KL divergence: $\int(\rho \log \rho + f\rho)dx.$	$\frac{1}{2}(2 + \log \rho + f - \mathbb{E}_\rho[\log \rho + f])(\Phi - \mathbb{E}_\rho[\Phi])\rho$ $-\frac{1}{2}(\mathbb{E}_\rho[\Phi(\log \rho + f)] - \mathbb{E}_\rho[\Phi]\mathbb{E}_\rho[(\log \rho + f)])\rho.$
Interaction energy: $\frac{1}{2} \int \int \rho(x)W(x, y)\rho(y)dxdy$	$\frac{1}{2}(W * \rho - \mathbb{E}_\rho[W * \rho])(\Phi - \mathbb{E}_\rho[\Phi])\rho$ $-\frac{1}{2}(\mathbb{E}_\rho[\Phi(W * \rho)] - \mathbb{E}_\rho[\Phi]\mathbb{E}_\rho[W * \rho])\rho$ $+(W * (\rho\Phi) - \mathbb{E}_\rho[W * (\rho\Phi)])\rho$ $-\mathbb{E}_\rho[\Phi]((W * \rho) - \mathbb{E}_\rho[W * \rho])\rho.$
Reverse KL divergence: $\int(\log \rho^* - \log \rho)\rho^*dx$	$\frac{1}{2}(\Phi - \mathbb{E}_{\rho^*}[\Phi])\rho + \frac{1}{2}(\Phi - \mathbb{E}_\rho[\Phi])\rho^*.$

TABLE 3. The formulation of $\mathcal{H}_E^F(\rho)$ under the Fisher-Rao metric.

Objective functional $E(\rho)$	$\mathcal{H}_E^W(\rho)\Phi$
KL divergence: $\int(\rho \log \rho + f\rho)dx.$	$\nabla^2 : (\rho \nabla^2 \Phi) - \nabla \cdot (\rho \nabla^2 f \nabla \Phi).$
Interaction energy: $\frac{1}{2} \int \int \rho(x)W(x, y)\rho(y)dxdy$	$-\nabla \cdot ((\nabla_{xy}^2 W * (\nabla \Phi \rho))\rho) - \nabla \cdot ((\nabla_{xx}^2 W * \rho_t)\rho \nabla \Phi).$
Reverse KL divergence: $\int(\log \rho^* - \log \rho)\mu dx$	$\nabla \cdot \left(\rho \nabla \left(\frac{\rho^*}{\rho^2} \nabla \cdot (\rho \nabla \Phi) \right) \right) + \nabla \cdot \left(\rho \nabla^2 \left(\frac{\rho^*}{\rho} \right) \nabla \Phi \right).$

TABLE 4. The formulation of $\mathcal{H}_E^W(\rho)$ under the Wasserstein metric.

for $k = 1$, we use the identity matrix I as the initial guess; for $k > 1$, we use S_{k-1} as the initial guess.

Algorithm 3 The CG method in the space of symmetric matrices.

Require: Operator $\mathcal{H} : \mathbb{S}^n \rightarrow \mathbb{S}^n$, $T \in \mathbb{S}^n$, initial guess $S^0 \in \mathbb{S}^n$, tolerance ϵ^{CG} , maximum iteration number K^{CG} .

- 1: Set $i = 0$. Let $R^0 = \mathcal{H}S^0 - T$ and $P^0 = -R^0$.
 - 2: **while** $i < K^{\text{CG}}$ or $\text{tr}((R^i)^2) > \epsilon^{\text{CG}}$ **do**
 - 3: Compute $\alpha^i = \frac{\text{tr}((R^i)^2)}{\text{tr}(P^i \mathcal{H} P^i)}$.
 - 4: Update $S^{i+1} = S^i + \alpha^i P^i$ and $R^{i+1} = \mathcal{H}S^{i+1} - T$.
 - 5: Compute $\beta^{i+1} = \frac{\text{tr}((R^{i+1})^2)}{\text{tr}((R^i)^2)}$.
 - 6: Update $P^{i+1} = -R^{i+1} + \beta^{i+1} P^i$.
 - 7: Set $i = i + 1$.
 - 8: **end while**
-

For the subproblem in Algorithm 2, the operator \mathcal{H} follows

$$\mathcal{H}S = 2S + (\bar{\Sigma}_k S F_k + F_k S \bar{\Sigma}_k),$$

and we have $T = \bar{T}_k$.